

FRESH APPROACH FOR HIGH-THROUGHPUT STUDIES OF ION-SELECTIVE  
MATERIALS USING REUSABLE CHEMFET PLATFORM

by

DOUGLAS HOWARD BANNING

A THESIS

Presented to the Department of Chemistry  
and the Graduate School of the University of Oregon  
in partial fulfillment of the requirements  
for the degree of  
Master of Science

March 2019

## THESIS APPROVAL PAGE

Student: Douglas Howard Banning

Title: Fresh Approach for High-Throughput Studies of Ion-Selective Materials Using Reusable ChemFET Platform

This thesis has been accepted and approved in partial fulfillment of the requirements for the Master of Science degree in the Department of Chemistry by:

Dr. Michael M. Haley	Chair
Dr. Darren W. Johnson	Advisor
Dr. Michael D. Pluth	Member

and

Janet Woodruff-Borden      Vice Provost and Dean of the Graduate School

Original approval signatures are on file with the University of Oregon Graduate School.

Degree awarded March 2019

© 2019 Douglas Howard Banning

## THESIS ABSTRACT

Douglas Howard Banning

Master of Science

Department of Chemistry

March 2019

Title: Fresh Approach for High-Throughput Studies of Ion-Selective Materials Using Reusable ChemFET Platform

Aqueous anions play an important role in our world, and the ability to continuously measure them provides both environmental and health benefits. Chemically-sensitive field effect transistors (ChemFETs) are becoming increasingly popular in the field of aqueous measurement due to their relatively low-cost capability for real-time, continuous sensing. Receptor molecules or mixtures displaying affinity for a particular ion can also be utilized in a ChemFET gate membrane. Receptors can be incorporated into the gate oxide membrane and the entire ChemFET can be utilized in an aqueous environment, thus utilizing hydrophobic receptors in an aqueous anion-sensing application.

Demonstrating the ability to reuse the sensors validates an important characteristic for ChemFET-based research. Additionally, numerous other receptor molecules are evaluated against an array of common anions. Selectivity coefficients are compared to the Hofmeister Series. Additional membranes are evaluated for suitability for incorporation of receptors on the ChemFET gate oxide surface. This thesis includes previously unpublished co-authored material.

## CURRICULUM VITAE

NAME OF AUTHOR: Douglas Howard Banning

### GRADUATE AND UNDERGRADUATE SCHOOLS ATTENDED:

University of Oregon, Eugene, OR  
Air Command and Staff College, Maxwell AFB, AL  
US Air Force Academy, Colorado Springs, CO

### DEGREES AWARDED:

Master of Science, Chemistry, 2019, University of Oregon  
Master of Arts, Organizational Leadership, 2016, ACSC  
Bachelor of Science, Materials Chemistry, 2009, USAFA

### PROFESSIONAL EXPERIENCE:

2<sup>nd</sup> Lt, USAF. Corrosion Engineer, Air Force Research Lab, Robins AFB, GA,  
2009-2011

1<sup>st</sup> Lt, USAF. Aircraft Structural Engineer, Tactical Airlift Division, Robins AFB,  
GA, 2011-2013

Capt, USAF. Flight Test Engineer/Instrumentation Flight Commander, Air Force  
Special Operations Command, Hurlburt Field, FL, 2013-2016

Capt, USAF. Flight Test Engineer/Vertical Lift Flight Commander, Air Force  
Special Operations Command, Hurlburt Field, FL, 2016-2017

Capt/Major, USAF. Student, University of Oregon, Air Force Institute of  
Technology/Civilian Institute Program, 2017-2019

### PUBLICATIONS:

Banning, D. H. *National Association of Corrosion Engineers* **2011**.

## ACKNOWLEDGMENTS

I first recognize God's continual faithfulness and blessing in my life far beyond what I imagined or deserve. I want to take this opportunity to thank my wife, Bethany, and my girls, Evelyn and Ingrid, who showed me an incredible amount of love and patience throughout this program. I owe my love of chemistry to my dad, Dr. Jeff Banning. I appreciate all of his mentoring and guidance, and in particular with chemistry, starting in high school all the way to undergrad at USAFA and then to graduate school. I would also like to recognize my mom as my first teacher, whose love and instruction instilled a love of learning that has served me my entire academic career. I would like to thank my parents as well as my siblings, whose prayer, love, and support has helped carry me through.

I wish to express my sincere appreciation to Professors Darren Johnson and Mike Haley for being such wonderful mentors and for being so accommodating with my AF program constraints; Darren as advisor, and Mike as my committee chair. In addition, a very special thanks are due to my mentor Dr. Sean Fontenot, who provided help and guidance over the course of my entire program. I would also like to take this opportunity to thank Professor Mike Pluth for serving on my committee, as well as each member of the DWJ group for their unwavering support and encouragement.

This is dedicated to my girls; Bethany, Evelyn, and Ingrid.

This project was supported in whole by the United States Air Force and the Air Force Institute of Technology's Civilian Institute Program. The views expressed in this thesis are those of the author and do not reflect the official policy or position of the United States Air Force, Department of Defense, or the U.S. Government.



## TABLE OF CONTENTS

Chapter	Page
I. INTRODUCTION.....	1
Introduction .....	1
ChemFETs.....	2
Figures of Merit.....	3
Sensitivity and Detection Limit.....	3
Selectivity .....	4
Shift in Y-Intercept.....	5
Applications.....	6
Drop Casting.....	7
II. RECYCLABILITY .....	9
Introduction .....	9
ChemFET Overview.....	10
EXPERIMENTAL SECTION.....	12
Reagents .....	12
Setup.....	12
Driver Circuit.....	12
ChemFETs.....	13
Device Testing.....	14
RESULTS AND DISCUSSION.....	14
Nitrate Sensitivity and Selectivity .....	14

Chapter	Page
Ammonium Sensitivity and Selectivity .....	17
Dihydrogen Phosphate Interference.....	18
Total-N Sensing .....	21
Conclusions .....	22
III. CHEMFET DATA.....	23
Introduction .....	23
Comparison of Receptor Performance.....	24
Core Protonation State .....	26
pH Sensitivity .....	31
Polyvinyl Chloride Membranes.....	35
pH Testing .....	36
Halogen-Bonding Receptors .....	44
Longevity and Storage .....	47
IV. CONCLUSION AND FUTURE DIRECTION .....	50
Conclusion.....	50
FUTURE DIRECTION.....	51
Design of Experiments.....	51
Plasticizer .....	51
Receptor and Ionic Additive.....	51
Structural DOE .....	52

Chapter	Page
Charged Receptors .....	52
Soil Evaluation.....	53
APPENDIX: CHAPTER II FIXED INTERFERENCE DATA.....	54
REFERENCES CITED.....	59

## LIST OF FIGURES

Figure	Page
1. UO Receptor Scaffold.....	1
2. ChemFET Diagram.....	2
3. Sensitivity and Detection Limit.....	3
4. Fixed Interferent Characterization.....	5
5. Drop Casting.....	7
6. Nikolsky-Eisenman Equation.....	11
7. Sensor Response vs Nitrate Activity.....	15
8. Selectivity Coefficients.....	16
9. Selectivity Coefficients compared to Hofmeister Series.....	17
10. Evidence of $\text{H}_2\text{PO}_4^-$ Dimerization.....	19
11. Phosphate Speciation Diagram.....	20
12. Total-N Separate Runs.....	21
13. Total-N Simultaneous Runs.....	22
14. Initial Receptor Scaffold.....	23
15. Nitrile Butadiene Rubber.....	23
16. NBR, Pyridinium Core, Nitro Shoes.....	24
17. NBR, Pyridine Core, Nitro Shoes.....	25
18. Core Protonation State Comparison.....	27
19. NBR, Pyridine Core, Methoxy Shoes.....	28
20. NBR, Bipyridine Core, Methoxy Shoes.....	29

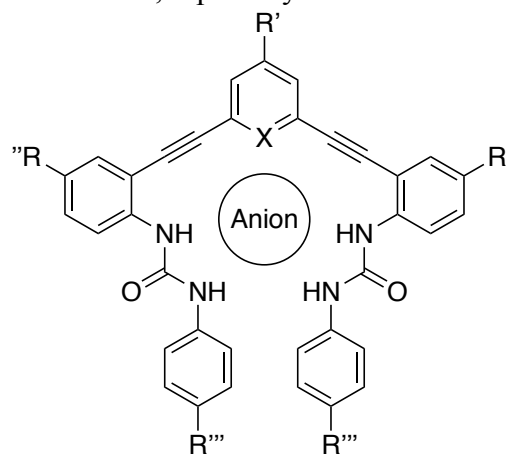
Figure	Page
21. NBR, TOAN, No Receptor .....	30
22. PolyHEMA Nitrate Sensitivity Comparison .....	32
23. PolyHEMA pH Sensitivity Comparison .....	33
24. TREN.MAM Receptor .....	34
25. TREN.MAM and TREN.IAM in Hydrogen Phosphate.....	34
26. Polyvinyl Chloride (PVC).....	35
27. ortho-Nitrophenyl Octyl Ether (NPOE).....	35
28. pH Testing of NBR vs PVC Membranes .....	36
29. PVC 65-NPOE, Pyridine Core, Methoxy Shoes .....	37
30. PVC 65-NPOE, Pyridinium Core, Nitro Shoes.....	38
31. PVC 65-NPOE, Pyridinium Core, Nitro Shoes, 1/10 TOAN .....	39
32. PVC 65-NPOE, TOAN, No Receptor .....	40
33. PVC 50-NPOE, Pyridinium Core, Nitro Shoes, No TOAN.....	41
34. PVC 50-NPOE, Bipyridine Core, Methoxy Shoes.....	42
35. PVC 50-NPOE, N-Confused N-Oxide Core, CF <sub>3</sub> Shoes.....	43
36. Halogen-Bonding Receptor .....	44
37. Halogen-Bonding Receptor in Chloride.....	45
38. Halogen-Bonding Receptor in Nitrate .....	46
39. Equilibration Curves for Wet ChemFET Storage.....	47
40. Equilibration Curves for Dry ChemFET Storage.....	48
41. Bromide 0.01M Fixed Interference.....	54
42. Sulfate 0.5M Fixed Interference .....	54

Figure	Page
43. Hydrogen Phosphate 1mM Fixed Interference.....	55
44. Perchlorate 0.01mM Fixed Interference.....	55
45. Chloride 1.5M Fixed Interference .....	56
46. Iodide 0.1mM Fixed Interference .....	56
47. Dihydrogen Phosphate 0.5mM Fixed Interference.....	57
48. Dihydrogen Phosphate 1M Fixed Interference.....	57
49. Fluoride 0.4M Fixed Interference.....	58

## CHAPTER I. INTRODUCTION

**Introduction.** Aqueous anions play an important role in our world. In an agricultural application, nitrates and phosphates are important plant nutrients. However, overapplication of some of these nutrients can be harmful to the environment. Overfertilization can lead to excess nitrates and phosphates in groundwater and other associated ecosystems. For example, overabundance of nutrients in lakes and rivers can cause problems like eutrophication and algal blooms. Water contamination by other anions like perchlorates can cause medical issues with the local populace.<sup>1</sup> The ability to measure anion concentration is vitally important in our world, especially in areas increasingly rife with pollution and runoff.

Much work has been done at the University of Oregon in the field of anion sensing, developing supramolecular “hosts” which house anionic “guests”. The collaboration between the Darren W. Johnson research group and Mike Haley research group has developed an arylolethynyl bisurea anion receptor scaffold which has been shown to act as a host for nitrate and phosphate guests (see



**Figure 1. UO Receptor Scaffold.** Arylolethynyl bisurea receptor scaffold. R' and X are in the "core," R" is termed "elbow," R'" is termed "shoe." Depicted with anion in the binding pocket. The binding pocket is comprised of five hydrogen-bond donors/acceptors; the four urea N-H hydrogen-bond donors, and X can represent an addition N-H or C-H hydrogen bond donor, or an N hydrogen bond acceptor.

Figure 1).<sup>2</sup> The modular approach to synthesizing this scaffold facilitates modification of three main functional areas: the “core,” the “elbows,” and the “shoes.” The varying functionality at these three points can tune the strength of the local hydrogen bond donors and/or acceptors to better bind to a targeted anion of interest. The binding of host to guest

in some cases can produce either on-to-off or off-to-on fluorescence.<sup>3</sup> Given the water insolubility of the receptor molecule, binding studies must be conducted in less polar solvents such as DMSO and chloroform.<sup>2,3</sup>

One of the difficulties with implementing this particular receptor scaffold in an aqueous anion sensing capacity is due to the practical insolubility of the receptor in water. However, non-water-soluble receptors are often suitable for use in the chemically selective materials (usually polymers) used in ion-selective electrodes (ISEs) and chemically-sensitive field effect transistors (ChemFETs).

**ChemFETs.** ChemFETs are becoming increasingly popular in the field of potentiometric sensing due to their relatively low-cost capability for real-time, continuous sensing.

ChemFETs are a subset of ion-sensitive field effect transistors, or ISFETs. An ISFET is a

transistor where the characteristics of the gate circuit are dependent on any ions present between the gate electrode and the gate oxide

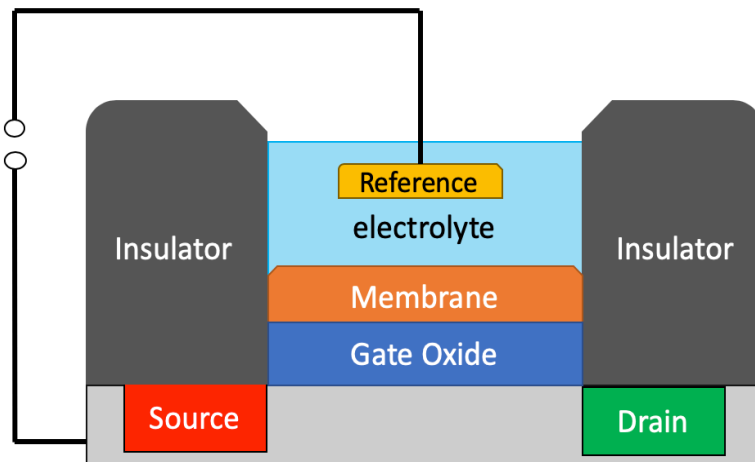


Figure 2. ChemFET Diagram. A concentration gradient between the analyte in the electrolyte solution and the membrane on the gate oxide creates a potential. This potential changes the characteristics of the source-gate circuit, which is measurable.

(see Figure 2). A

ChemFET

introduces a barrier on the gate oxide that imparts some level of selectivity, where only specific ions in the electrolyte or analyte solution affect the gate circuit. ChemFETs utilize a semi-permeable membrane applied to the gate electrode surface, containing a



receptor with selective affinity to an analyte of interest. The affinity of the target analyte of interest to the receptors embedded in the gate membrane creates a concentration gradient between the membrane and the solution being analyzed. The imbalance of charged species creates a chemical potential between the sample and the gate oxide, changing the characteristics of the gate circuit. This effect on the gate circuit imparted by the sample is measurable and relates to analyte concentration in the sample.<sup>4</sup>

**Figures of Merit.** There are three major figures of merit that are of significance to ChemFET measurements; detection limit, sensitivity, and selectivity.

**Sensitivity and Detection Limit.** The sensitivity and detection limit of the sensor are

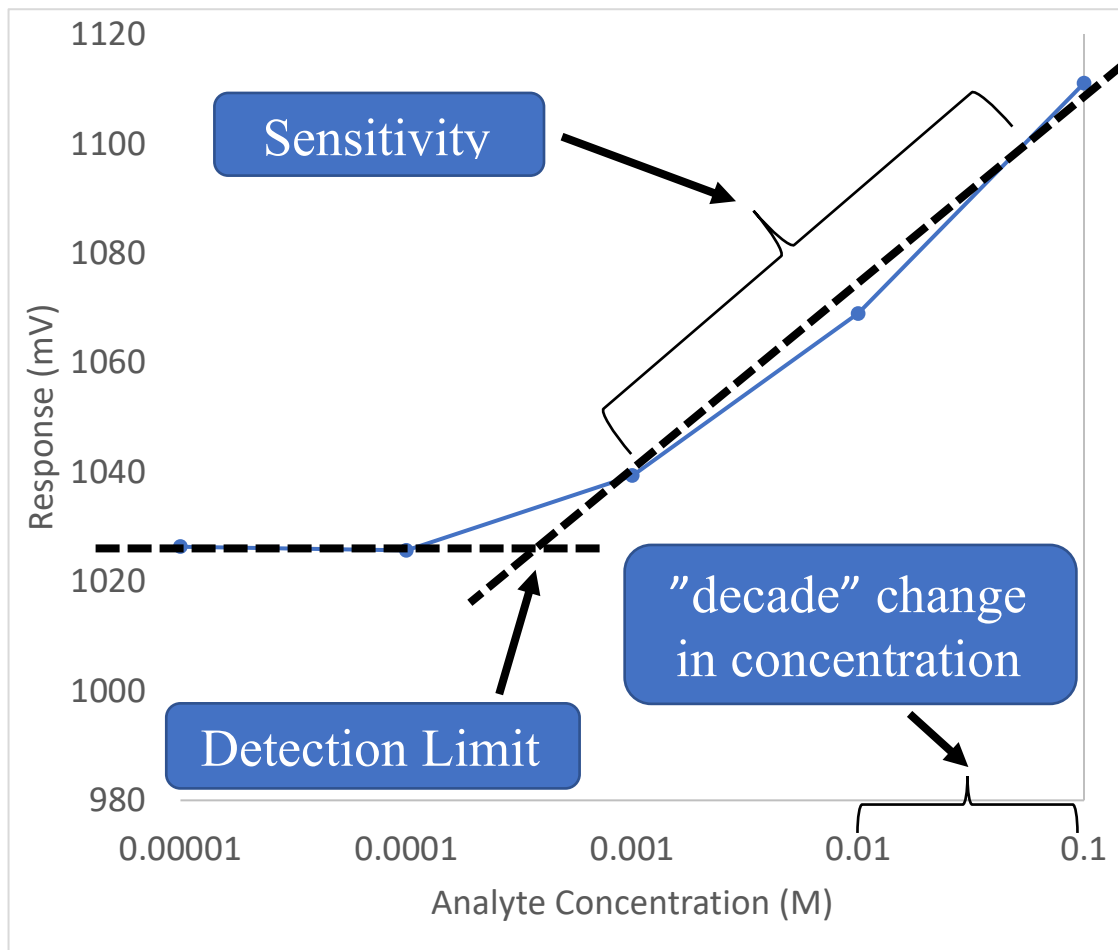


Figure 3. Sensitivity and Detection Limit. The slope of the measurement indicates the sensitivity of the method. The detection limit shows the point at which the analyte is no longer detectable over the background.

measured by the curve generated by FET response as a function of concentration. The detection limit represents the lowest concentration of the target analyte that can be measured above the background noise of the system. Sensitivity is measured by the slope of ChemFET response (commonly reported in volts or millivolts) as a function of analyte concentration. Greater sensitivity translates to a smaller change in concentration producing a measurable change in response, or correspondingly a larger response for a given change in concentration. Slope is generally reported in units of millivolts (or volts) per order of magnitude change in concentration, termed “decade” (see Figure 3). The steeper the slope, the larger the electronic response to a given change of concentration and therefore the greater the sensitivity of the sensor to concentration of analyte.

Generally, our devices show positive signal response to anions. In other words, the gate voltage increases as anion concentration increases, resulting in a positive slope in the reading. The opposite response is usually observed for cations. For example, for our ammonium-selective devices, signal decreases as cation concentration is increased, resulting in a negative slope in the reading.

**Selectivity.** Selectivity represents the ability of the sensor to measure the concentration of the desired target analyte in the presence of interfering ions. Selectivity can be measured using either the Separate Solution Method (SSM) or the Fixed Interferent (FI) method. Both SSM and FI characterizations report a series of selectivity coefficients for various competing ions, which are a quantitative depiction of the sensitivity of the method to distinguish between the target analyte and the single interferent.

The SSM method entails running the sensor through a solution of the target analyte A (with no interferent B), and then run again in a solution of interferent B (with

no analyte A). Both responses are then combined to report a coefficient describing how sensitive the method is to a particular interferent in relation to the target analyte.

The FI method involves measuring a series of solutions that combine a varying target analyte concentration and fixed interferent concentration. The selectivity coefficient is calculated from the point where the flat interferent line intersects the target

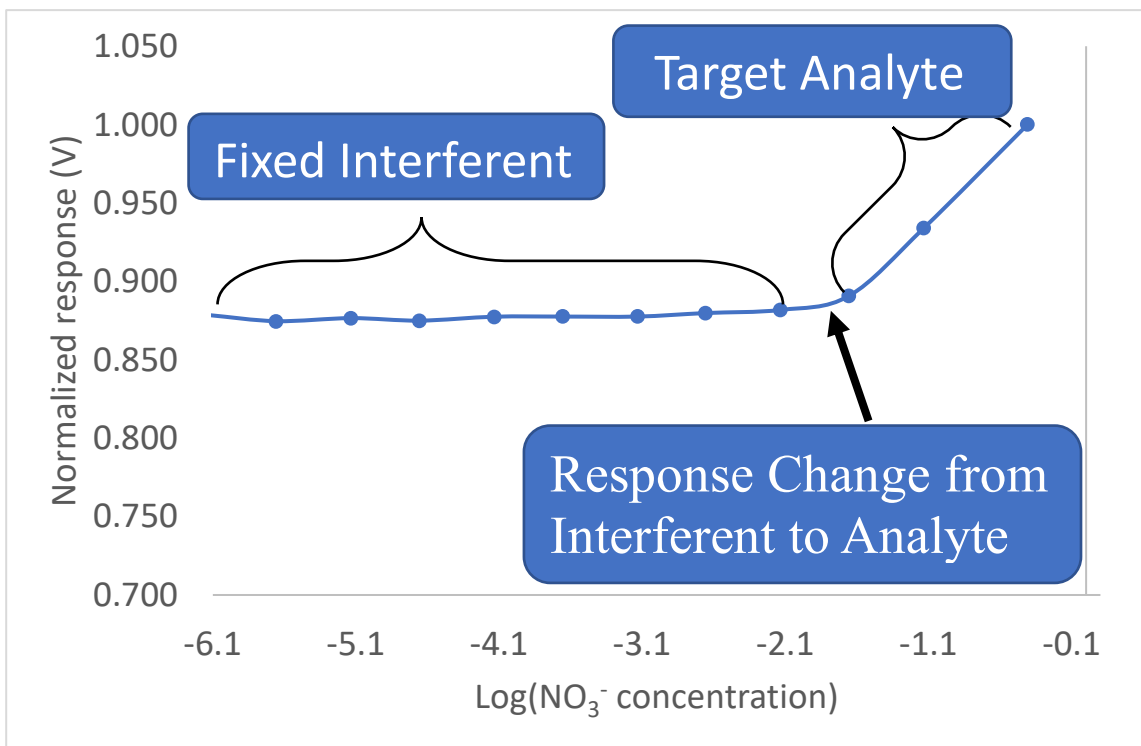


Figure 4. Fixed Interferent Characterization. The response at lower concentrations of analyte is clearly dominated by interferent. The selectivity coefficient is calculated from the bend in the curve where the response changes from interferent to analyte.

analyte line (see Figure 4).

The FI method produces selectivity coefficients that are considered more reliable, as the method involves measurements taken with both the primary and interfering ions in the same solution.

**Shift in Y-Intercept.** The y-intercept can vary sensor to sensor; testing has demonstrated that it does not affect the sensitivity. There is no useful information contained in the y-

intercept of the measurement; any differences come from manufacturing tolerances as well as slight variances in the summed junction potentials of each solid-liquid interface. These junction potentials vary with interface surface area and shape.<sup>5</sup> This allows for responses to be normalized to a response value for easier graphical comparison.

**Applications.** A significant application of ChemFETs is in the area of real-time ion sensing. Receptor molecules or mixtures with affinity for particular anions can be integrated within a membrane on top of the gate oxide to provide selectivity for ionic analytes. Since the ChemFET works by converting molecular recognition to a measurable signal, one advantage to ChemFET sensors is that no visual indicator is necessary as is common in many other guest-host evaluations (such as off-to-on or on-to-off fluorescence).<sup>3</sup> This is particularly useful when dealing with applications where optical indicators cannot be distinguished, such as in turbid samples. The continuous response of ChemFET-based sensing allows for real-time information to be collected on the analyte of interest. Embedding the receptor in the membrane on the gate allows the use of non-water-soluble receptors to be applied in aqueous ion sensing applications without having to connect these receptors to the material via covalent bonds. Other research groups working with ChemFETs use various membranes for controlling the chemical interactions on the gate oxide surface such as polysiloxane and polyacrylamide.<sup>7,8</sup> We drop cast the NBR membrane with embedded receptor and additives directly on the gate oxide.

**Drop Casting.** The ChemFETs are coated via drop casting (see Figure 5). The DWJ lab has developed a modular drop casting method allowing for easy drop-in replacement of individual components for easy change of components. There are four categories of drop cast stock solutions, each containing one component of the overall membrane and all are in the same solvent. The first drop cast stock solution contains the receptor molecule or cocktail. The second drop cast stock solution contains the membrane (sometimes with plasticizer). The third stock solution is for any ionic additive (often TOAN) being introduced to modify the membrane character. The fourth stock solution is a test aliquot dedicated for testing any other components (such as secondary receptors or ionic additives), and is

often left blank (just solvent). A sensor drop cast solution is created by measuring equal aliquots from one each of the four stock solution

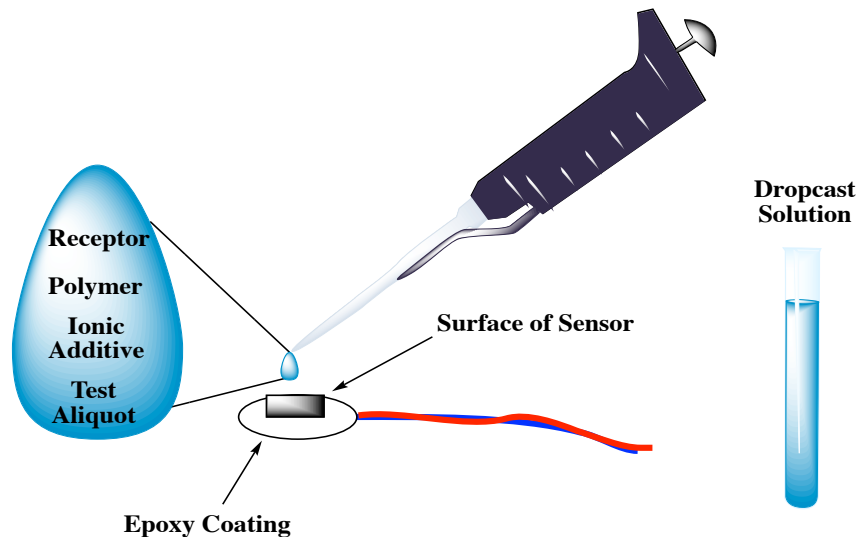


Figure 5. Drop Casting. The four-part solution contains receptor, any ionic additives, membrane and any plasticizer, and a test aliquot.

categories. This modular approach facilitates high-throughput testing. When, for instance, testing new membranes, existing receptor and additive stock solutions can still be used. The only new solutions that are needed are those containing new components under evaluation. Reducing the number of measurements here reduces probability of error as well as eases overall workload in the lab.

Off-the-shelf ISE receptor mixtures displaying ion affinity can also be utilized in a ChemFET gate membrane. One benefit of using off-the-shelf receptors is that it removes a variable when attempting to characterize ChemFETs for a particular use-case. We used off-the-shelf Sigma Aldrich (SA) nitrate and ammonium receptor cocktails designed for ISEs for our initial ChemFET characterization, which removed an unknown that would have otherwise been present by utilizing experimental receptor systems. We used these off-the-shelf systems to develop and validate a recyclable and high-throughput platform for testing different polymer membrane receptor formulations. The portion of chapter II directly relating to recyclability was included in previously unpublished co-authored material.

## CHAPTER II. RECYCLABILITY

Portions of this chapter were co-authored by Sean A. Fontenot, Darren W. Johnson, Julia M. Fehr, and Ian S. Torrence from the Department of Chemistry, University of Oregon, and Jordan R. Kusiek, Andreas M. Wenzel, and Calden N. Carroll from SupraSensor Technologies. Sean Fontenot provided writing and editorial assistance. Julia Fehr and Ian Torrence performed some of the lab experiments. Doug Banning prepared the chapter, contributed to each section, provided most of the material, performed literature research and analysis, and compiled material from the other authors. Excerpts from this chapter will be submitted to *ACS Sensors* under the title “Demonstrating the Recyclability of ChemFETs and use as a Total Nitrogen Sensor.”

**Introduction.** Off-the-shelf ISE receptor mixtures displaying analyte affinity can also be utilized in the gate oxide membrane of a ChemFET. The receptor mixtures embedded in the polymer membrane make the membrane selective for an analyte. One benefit of using off-the-shelf receptors is that it removes a variable when attempting to characterize ChemFETs for a particular use-case. Use of Sigma Aldrich (SA) nitrate and ammonium receptor cocktails allowed for initial ChemFET characterization by removing an unknown factor that would have otherwise been present by utilizing DWJ lab-developed receptors. Full characterization of the ChemFET setup using known and proven receptor systems allowed additional factors to be explored without potential confounding by untested or experimental receptor systems. Recyclability was the factor of interest in this study. Recyclability of ChemFETs is the ability to strip the selective membrane from the

gate oxide, reapply a different selective coating, and observe the device change characteristics. We picked out off-the-shelf ChemFETs, polymers, deposition method and used an off-the-shelf nitrate receptor cocktail designed for ISEs along with another literature-derived formulation for an ammonium ChemFET and developed and validated a recyclable and high-throughput platform for testing different polymer membrane formulations.

**ChemFET Overview.** ChemFETs are attractive as ion-sensing devices due to their low cost, low power consumption, and capability for continuous measurement. Like ISEs, ChemFETs rely on ion-selective materials, usually polymers, to regulate the interfacial potential between the analyte sample solution and the gate oxide (or the filling solution in the case of ISEs).

Ideally, an ion-selective material can be applied such that this interfacial potential is dependent only on the activity of a target analyte. This potential can then be measured and taken as a signal corresponding to activity of the target analyte. Many excellent articles further describe the functional principles of ChemFETs.<sup>4,7,11,12</sup> In practice, the interfacial potential between the sample environment and gate oxide of the ChemFET is convoluted with several other interfacial potentials and perfect selectivity of a material for one target analyte is not often achievable.<sup>5</sup> The variance in the interfacial potentials affects the response voltage, which translates to varying y-intercepts when graphing different ChemFET responses. In order to deconvolute the potential generated by interactions with the target analyte from other changes in measured potential, the ChemFET devices must be evaluated in terms of three key figures of merit: sensitivity, detection limit, and selectivity.



The sensitivity of the ChemFET is defined by the slope obtained when the signal is plotted vs the logarithm of the activity of the target analyte. Ideal sensitivity, the maximum sensitivity achievable by potentiometric devices, is described by the Nernst equation expressed as 59 mV per decade.

The detection limit represents the lowest amount of analyte distinguishable from the background noise of the system, and is calculated from the bottom of the sensitivity slope.

Selectivity describes the ability of the sensor to distinguish the target analyte, A, from specific interfering species, B. Selectivities are represented by selectivity coefficients which are generally expressed as  $K_{A,B}^{pot}$  as defined by the Nikolsky-Eisenman equation (Figure 6).<sup>6</sup> Small values of  $K$  indicate a greater selectivity for the target analyte, A. Large values of  $K$  indicate a greater selectivity for the interferent, B. Selectivity coefficients are best determined by the fixed interference (FI) method.

$$K_{A,B}^{pot} = \frac{a_A}{a_B^{Z_A/Z_B}}$$

Figure 6. Nikolsky-Eisenman Equation. A is analyte, B is interferent.  $K_{A,B}^{pot}$  is the potentiometric selectivity coefficient for interferent B with respect to the analyte A,  $a_A$  is activity of A,  $a_B$  is activity of B,  $Z_A$  is charge of A, and  $Z_B$  is charge of B.

One way to prepare an ion-selective material is to incorporate molecules having ion-selective functionality into a polymer membrane which is then applied to the gate oxide. In this way, the ChemFET converts molecular recognition events in the polymer membrane to a measurable signal. It is important to note that the interactions between the polymer membrane and target analyte must be reversible.

When being used to screen potential ion receptors and their corresponding ion-selective materials, there is a significant advantage in the ability to “recycle” the ChemFET substrate. In terms of both cost and preparation effort, the ChemFET substrate

is generally the most expensive component of the device. Therefore, the cost of research and development may be reduced if substrates are reusable over tests involving several different configurations and material formulations. Cost and labor savings combine to enable higher throughput screening of devices. There is a further experimental advantage of insuring that a device's behavior be strictly tied to the polymer/material formulations.

Additionally, there is an urgent need to utilize real-time sensors to detect both the nitrate and ammonium concentration of soil in agricultural applications, a measurement termed "total-N" content of the soil.<sup>15</sup> Therefore, we demonstrate this process in the context of developing sensors for total-N measurement.

## EXPERIMENTAL SECTION

**Reagents.** The receptor membranes were composed high molecular weight polyvinyl chloride (PVC) (SA product 81387) with 35% by weight nitrophenyl octyl ether (NPOE) (Fluka product 73732) acting as plasticizer. For nitrate detection the SA nitrate ionophore cocktail A (SA product 72549) was used. For ammonium detection the SA ammonium receptor (SA product 09877) was used along with potassium tetrakis (4-chlorophenyl) borate (SA product 60591). The solvent used was anisole (Fluka product 10530). All reagents were used without purification unless otherwise noted. All analytes were analytical grade purchased from TCI Chemicals and Sigma Aldrich.

**Setup.** FET substrates were purchased from Winsense<sup>TM</sup>. The experimental setup consisted of driver circuit, up to four ChemFETs, a single Ag/AgCl reference electrode, and a data acquisition unit.

**Driver Circuit.** The driver circuit uses an instrumentation amplifier to drive the source to drain voltage ( $V_{DS}$ ) of the ChemFET at 617.5 mV and the drain current at 99.6  $\mu$ A. The

circuit keeps the external reference electrode at ground while the voltage between source and ground ( $V_{GS}$ ) is changed in order to maintain the above current and voltages.  $V_{GS}$  is taken as the measurement signal. The entire circuit is doubled to allow an array of two sensors to operate with the same reference electrode (the same ground). Several sets of these circuits may be run simultaneously, all using the same reference electrode.

The analog output of the driver circuit was recorded using an NI-DAQ 6009 data acquisition unit connected to a Windows™ computer and operated by a custom LabView™ program. The signal was recorded at a rate of 1 kHz. Each measurement was taken as the average of the signal over the last second of the 5-minute measurement.

**ChemFETs.** ChemFETs were purchased from Winsense™ having been wirebonded to small printed circuit boards and having their source and drain electrically accessible through small vias. Wires were soldered to these vias to allow remote connection to the source and drain and then the exposed connections were coated with Loctite marine epoxy. Then, polymer membranes were drop cast onto the ChemFET surface. During all drop cast processes, fourteen 1.6  $\mu$ L drops of the drop-cast solution were applied to the ChemFET surface spaced 15 minutes apart to allow for the solvent to evaporate. Following the drop-cast the sensors were placed in an oven at 80° overnight to facilitate complete evaporation of any remaining solvent.

*Formulation A*, when cast onto the ChemFET surface, yields a nitrate selective ChemFET. The drop cast solution was prepared by dissolving 0.0261 g SA nitrate ionophore cocktail A, 325 mg PVC, and 175 mg NPOE plasticizer in 20 mL anisole.

*Formulation B*, yields a PVC membrane containing only PVC and NPOE. This was prepared with 325 mg PVC, and 175 mg NPOE plasticizer in 20 mL anisole.

*Formulation C*, used for ammonium ChemFETs was prepared similarly to *A*. 2.8 mg nonactin, 26.5 mg potassium tetrakis (4-chlorophenyl) borate, 435 mg PVC and 236 mg NPOE were dissolved in 20 mL in anisole.

To recycle the ChemFETs, the sensors were soaked in ethanol for 5 minutes and the PVC coatings were removed by careful wiping with a Kimwipe. Bare ChemFETs were soaked 30% H<sub>2</sub>O<sub>2</sub> for 30 minutes then rinsed with deionized (DI) water followed by ethanol, and then dried. Following drying, fresh membranes could be cast onto the ChemFETs.

**Device Testing.** Each test involved a set of four identical ChemFETs and triplicate runs in which the first and last runs were performed from high to low concentrations while the second run was always performed from low to high. Measurement times were 5 minutes and all sensors and reference electrodes were rinsed with DI water between measurements. Before each test, ChemFETs and reference electrodes were preconditioned by soaking solutions having the highest target analyte solution for the series for 30 minutes prior to each run. Following preconditioning, the sensors were rinsed in DI water.

## RESULTS AND DISCUSSION

**Nitrate Sensitivity and Selectivity.** When formulation A is applied to the gate oxide, the gate voltage is dependent on nitrate activity and increases with nitrate activity. The average detection limit for the set of four sensors was found to be 3.1 mM in when measuring sodium nitrate in DI water (Figure 7). From the same experiment, the average sensitivity was found to be 40 mV/decade. When the polymer membrane from

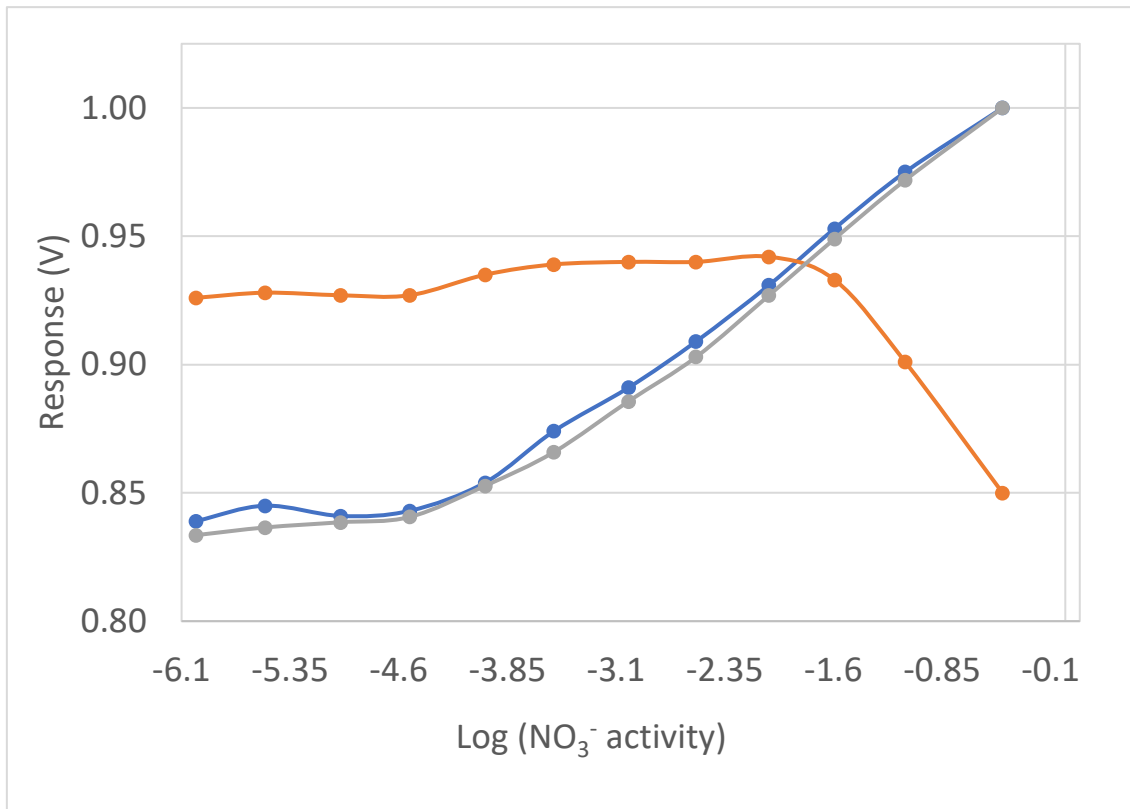


Figure 7. Sensor Response vs Nitrate Activity. Blue indicates fresh ChemFETs with SA nitrate selective receptor embedded in the gate oxide membrane. Red indicates the first recycling event of nitrate selective membrane removed and replaced with a blank polymer membrane. Grey indicates the second recycling event, returning the nitrate selective membrane and restoring nitrate response. Davies activities were calculated from the concentrations of each solution.

formulation A was replaced by formulation B, which contained only PVC and plasticizer, most of the sensitivity to nitrate was removed except at higher concentration. At higher concentrations, we observed that the dependence on sodium nitrate was such that the gate voltage *decreased* as activity *increased*. After removing these membranes and replacing with fresh membranes from formulation A, the original nitrate-sensitive behavior was restored. For these twice-recycled devices, the average sensitivity and selectivity were found to be 3.6 mM and 44 mV/decade respectively, acceptably close to those of the original set of devices. Since eliminating the SA nitrate ionophore cocktail from the membrane formulation effectively removed sensitivity to nitrate, the response to nitrate

may be attributed to the SA nitrate ionophore cocktail and not to the polymer or plasticizer.

Selectivity coefficients in Figure 8 were determined for common anions using the FI method. Ranking the potential interferents in terms of their interfering ability reveals a Hofmeister-like trend that holds across all devices referenced in Figure 7. The challenge

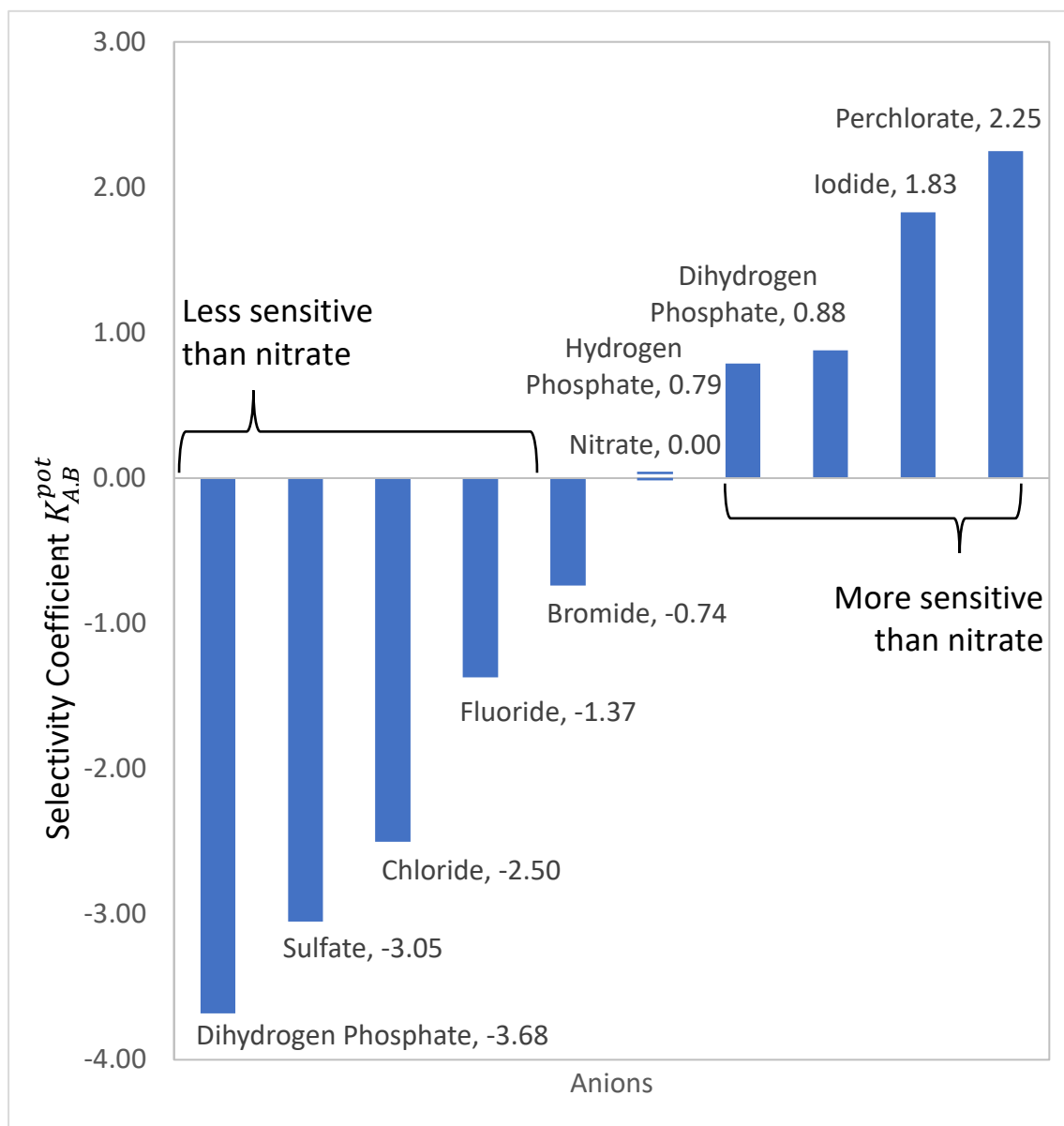


Figure 8. Selectivity Coefficients. Graph of selectivity coefficients  $K_{A,B}^{pot}$ , where A is  $\text{NO}_3^-$  and B is the interferent. The selectivity coefficient of  $\text{NO}_3^-$  is 0.0 by definition.

for those seeking to improve selectivity is not only to lower selectivity coefficients but to alter the selectivity profile of the material to such an extent that it rearranges this Hofmeister-like ranking such that, for example, nitrate switches places with perchlorate. The comparison of selectivity coefficients is presented in comparison to the Hofmeister series in

Figure 9.<sup>16</sup>

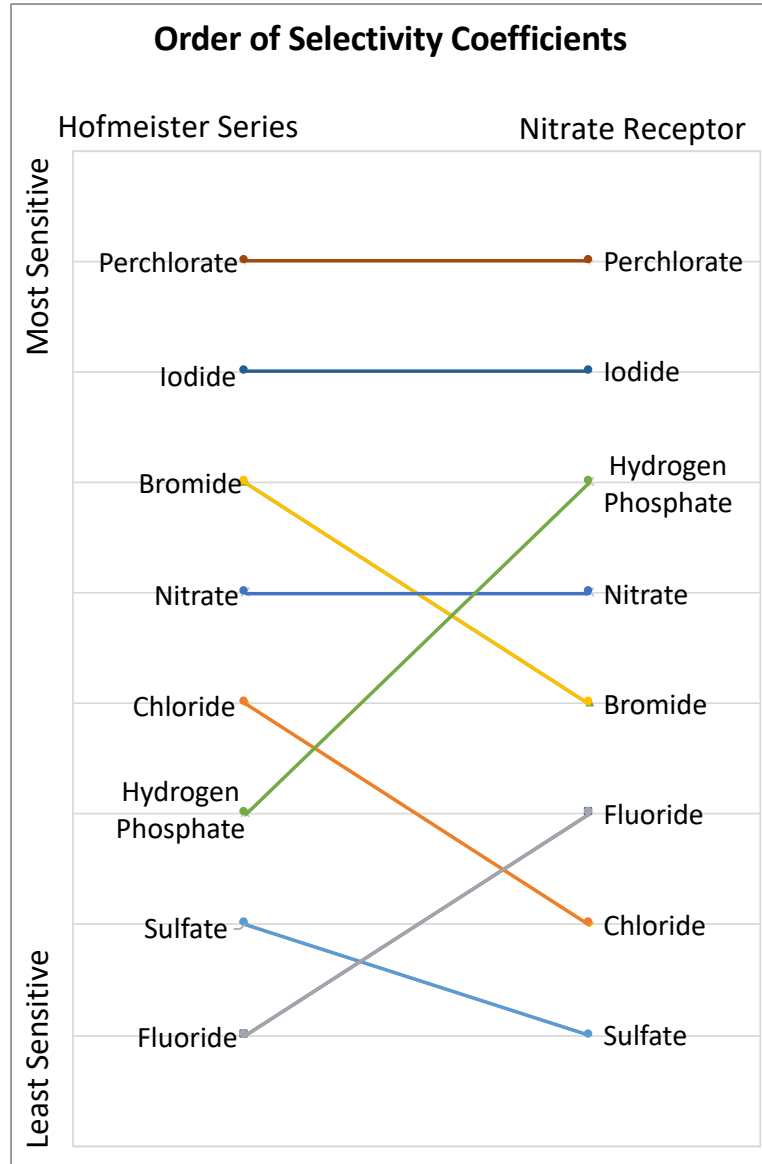


Figure 9. Selectivity Coefficients compared to Hofmeister Series. The selectivity coefficients calculated are ordered and compared to the Hofmeister series. Of particular interest are  $\text{HPO}_4^{2-}$  and  $\text{F}^-$  that increased in sensitivity from what would otherwise be expected per the Hofmeister ranking.

**Ammonium Sensitivity and Selectivity.** When formulation C is applied to the gate oxide, the gate voltage is dependent on ammonium activity and decreases ammonium activity increases. Average detection limit and sensitivity were found to be 4.5 mM and -37 mV/decade respectively. Ammonium ChemFETs could be recycled via the same

process described above. Eliminating potassium tetrakis (4-chlorophenyl) borate and the ammonium ionophore, nonactin, from the material limited the ChemFET sensitivity to ammonium. Therefore, we conclude that the nonactin and potassium tetrakis (4-chlorophenyl) borate are responsible for the bulk of the ammonium sensitivity and that the polymer and plasticizer contribute little in in this regard.

**Dihydrogen Phosphate Interference.** Typically, the interfering ability of an ion is independent of its activity. In other words, a fixed interferent experiment should yield the same selectivity coefficient regardless of the activity chosen for the interferent. In practice, a concentration must be such that interference is observed at sufficiently high target/analyte concentrations that it can be clearly distinguished from the detection limit of the target (nitrate, in this case). However, we observe significantly higher  $\text{H}_2\text{PO}_4^-$  interference at low concentrations (0.5mM) than higher concentrations (1M). Thus, we report two different selectivity coefficients in Figure 8. At concentrations near the solubility limit of  $\text{H}_2\text{PO}_4^-$ , approximately 2M, we observe no interference, so a maximum selectivity coefficient was calculated based on the detection limit. Previous studies involving  $\text{H}_2\text{PO}_4^-$  suggested some complicating factor resulting in a negative slope of response (in mV) as a function of concentration, in stark contrast to all other evaluated anions which produced a positive slope. We theorized dimerization may be the cause. The inverse slope suggested highest concentration of the unbound anion at lower overall  $\text{H}_2\text{PO}_4^-$  concentration. Work by Ceretta and Berglund indicated primarily free  $\text{H}_2\text{PO}_4^-$  at concentrations below 0.05M, and primarily oligomers present above 0.05M.<sup>10</sup> This is an entropic effect where higher extent of dimerization is observed at higher concentrations



(and thus fewer unbound species), and a lower extent of dimerization is observed at lower concentrations (and thus more unbound species).

To gain a better understanding of the role of  $\text{H}_2\text{PO}_4^-$  as an interferent, we further investigated the behavior of ChemFETs in  $\text{H}_2\text{PO}_4^-$  alone (Figure 10). We hypothesize that

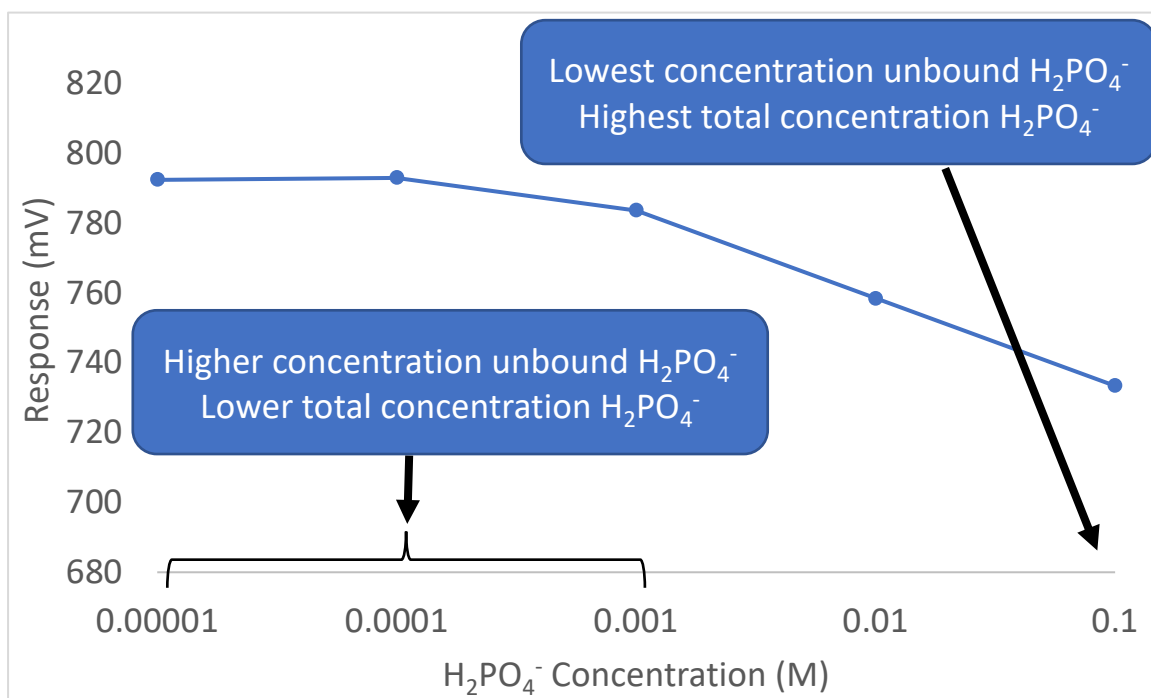


Figure 10. Evidence of  $\text{H}_2\text{PO}_4^-$  Dimerization? This graph depicts a run of ChemFETs with SA nitrate receptor in  $\text{H}_2\text{PO}_4^-$  with no interferents. We observe an inverse trend for  $\text{H}_2\text{PO}_4^-$  than we do for most other ions evaluated. We theorized that this effect was due to more unbound species at lower overall concentration, and fewer unbound species at higher concentration. If the ChemFET measures only unbound  $\text{H}_2\text{PO}_4^-$ , the speciation hypothesis would explain the inverse slope.

only the unbound  $\text{H}_2\text{PO}_4^-$  species acts as an interferent and therefore,  $\text{H}_2\text{PO}_4^-$  might demonstrate more interference at lower concentrations. If the ChemFET is only reporting the concentration of free or unbound  $\text{H}_2\text{PO}_4^-$ , the negative slopes may be easily explained since the concentration of unbound  $\text{H}_2\text{PO}_4^-$  is theoretically highest at the lowest overall  $\text{H}_2\text{PO}_4^-$  concentration, and lowest at the highest overall  $\text{H}_2\text{PO}_4^-$  concentration. There are numerous examples in Chapter III of sensors demonstrating a negative slope in response

to increasing  $\text{H}_2\text{PO}_4^-$  concentration, where nearly all other evaluated anions demonstrate a positive response.

To help support the hypothesis that  $\text{H}_2\text{PO}_4^-$  was the interferent species and  $\text{H}_2\text{PO}_4^-$  dimerization was the complicating factor, we needed to measure the pH of all phosphate interferent  $\text{NO}_3^-$  solutions to see if they fell within the range where phosphate exists in the  $\text{H}_2\text{PO}_4^-$  species. We consulted a speciation diagram and compared pH of the entire range of  $\text{H}_2\text{PO}_4^-$  interferent in  $\text{NO}_3^-$  solutions we evaluated to ensure the phosphate was in the  $\text{H}_2\text{PO}_4^-$  state in all cases. The solutions measured were the low and high  $\text{NO}_3^-$  solutions at the low  $\text{H}_2\text{PO}_4^-$  fixed level (0.5mM  $\text{H}_2\text{PO}_4^-$ ), and the low and high  $\text{NO}_3^-$  solutions at the high  $\text{H}_2\text{PO}_4^-$  fixed level (1M  $\text{H}_2\text{PO}_4^-$ ). The entire pH range of solutions tested was 4.03 to 5.64. Figure 11 indicates that all solutions measured contained phosphate in the  $\text{H}_2\text{PO}_4^-$  state.

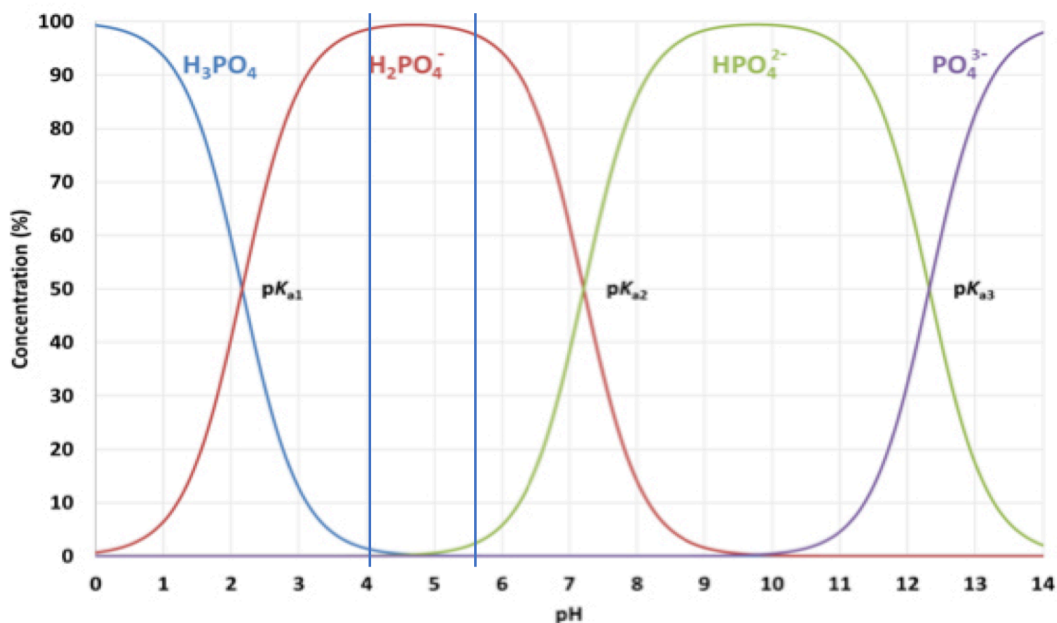


Figure 11. Phosphate Speciation Diagram. Measured pH of the  $\text{H}_2\text{PO}_4^-$  interferent  $\text{NO}_3^-$  solutions ranged from 4.03 to 5.64 (indicated by blue lines). The speciation diagram demonstrates everything within this pH range exists as predominantly the  $\text{H}_2\text{PO}_4^-$  species. Image retrieved from <http://ixora.pro/phosphoric-acid-dissociation>.

**Total-N Sensing.** In the course of addressing the challenge of total-N measurement, we evaluated whether  $\text{NO}_3^-$  and  $\text{NH}_4^+$  sensors may be operated simultaneously and thus allow for an accurate total-N measurement from a single experiment.<sup>15</sup> Figure 12 shows results of the  $\text{NO}_3^-$  and  $\text{NH}_4^+$  sensors run separately.

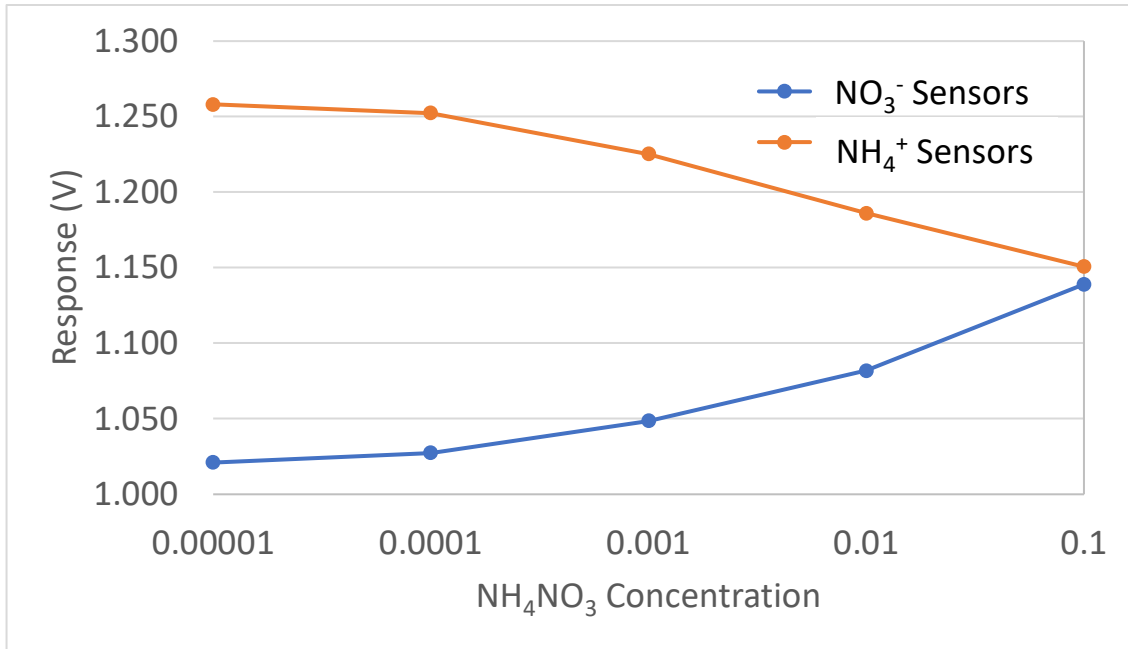


Figure 12. Total-N Separate Runs. The  $\text{NO}_3^-$  ChemFETs were tested for response to  $\text{NH}_4\text{NO}_3$ , with a positive response observed. The  $\text{NH}_4^+$  ChemFETs were then tested for response to  $\text{NH}_4\text{NO}_3$ , with a negative response observed.

Figure 13 shows results of the  $\text{NO}_3^-$  and  $\text{NH}_4^+$  sensors run simultaneously.

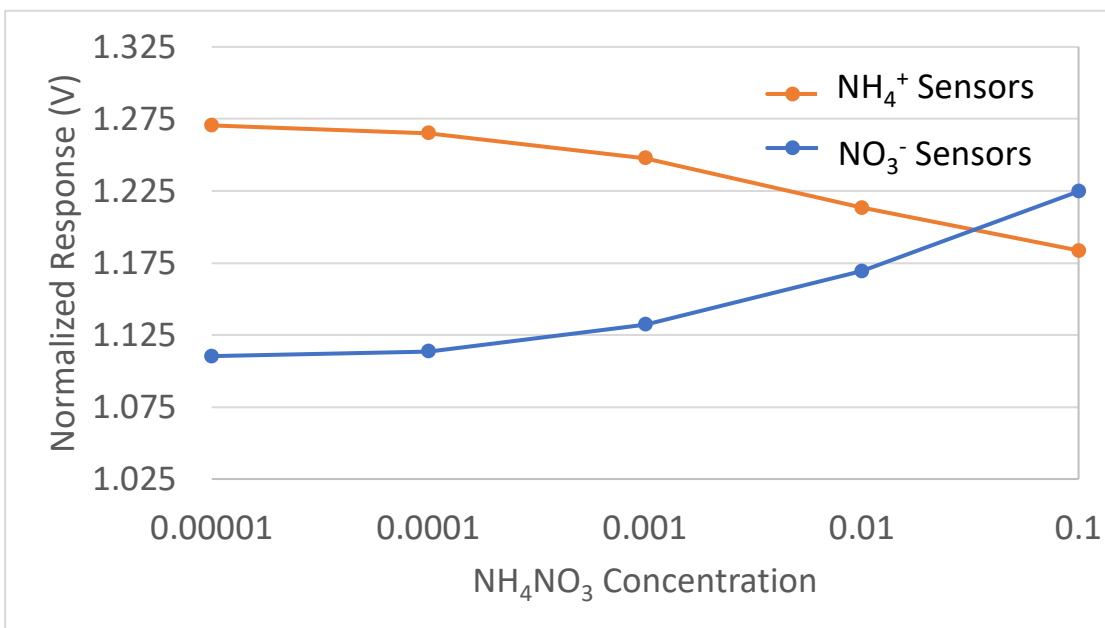


Figure 13. Total-N Simultaneous Runs. The  $\text{NO}_3^-$  and  $\text{NH}_4^+$  ChemFETs were simultaneously tested for response to  $\text{NH}_4\text{NO}_3$ . The  $\text{NO}_3^-$  ChemFETs displayed a positive response, and the  $\text{NH}_4^+$  ChemFETs displayed a negative response.

We observe that operating both sets of sensors in parallel has no negative impact on the performance of either set of sensors. Therefore, the simultaneous ( $\text{NO}_3^-$  and  $\text{NH}_4^+$ ) sensors device configuration can be applied to total-N measurement.

**Conclusions.** Nitrate and ammonium sensors were prepared based on accessible components/chemicals and were shown to have selectivity profiles similar to similar systems previously-reported.

We have demonstrated a platform that is reusable. Additionally, we have shown that our system can operate several ChemFETs simultaneously. We suspect this is not a unique advantage although it is rarely utilized for total-N measurement.

### CHAPTER III. CHEMFET DATA

**Introduction.** The receptor scaffold used in the majority of these studies was characterized in binding characterization studies by the anion sensing collaboration between DWJ and Haley research groups (Figure 14).<sup>2</sup> We chose several receptors with the same scaffold which were found to have an affinity for anions of interest (often  $\text{NO}_3^-$  or  $\text{HPO}_4^{2-}$ ) and incorporated those receptors into polymer membranes. The polymer membrane

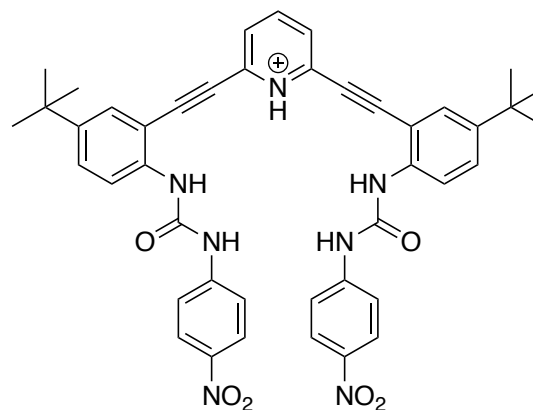


Figure 14. Initial Receptor Scaffold. Pyridinium core, t-butyl elbows, and nitro shoes. Additional scaffolds with modified functionality were evaluated.

we began with was nitrile butadiene rubber (NBR) (Figure 15).

We found it necessary to add tetraoctylammonium nitrate (TOAN) to the polymer membrane in order to achieve responsive sensors. In similar work involving anion-

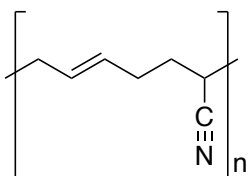


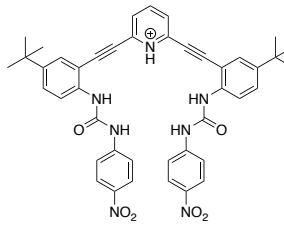
Figure 15. Nitrile Butadiene Rubber. NBR used as the gate oxide membrane.

selective ChemFETs, Reinhoudt and others found TOAN necessary to add immobile counterions to the membrane.<sup>6</sup> This is generally believed to facilitate anion mobility into the material.<sup>6</sup>

The composition of the membrane was 94.5 weight % NBR, 5 wt. % ionic additive TOAN, and 0.5 wt. % receptor. Any variation

will be noted respective to this default composition; for example, 1/10 TOAN represents 0.5 wt. % TOAN in the membrane.

**Comparison of Receptor Performance.** The following charts depict performance and observations of varying receptors, with detection limits and sensitivities reported where applicable.

Core:	Pyridinium	Detection Limits (mM): NO <sub>3</sub> <sup>-</sup> : 2.8 H <sub>2</sub> PO <sub>4</sub> <sup>-</sup> : 3.2	Sensitivity (mV/decade): NO <sub>3</sub> <sup>-</sup> : 49 H <sub>2</sub> PO <sub>4</sub> <sup>-</sup> : -38	
Elbows:	t-butyl			
Shoes:	Nitro			

ChemFETs were coated with NBR membrane containing TOAN and receptor. The receptor used had a pyridinium core, t-butyl elbows and nitro shoes. The ChemFETs were tested for response to NO<sub>3</sub><sup>-</sup> and H<sub>2</sub>PO<sub>4</sub><sup>-</sup>. In these experiments we observed a positive response to NO<sub>3</sub><sup>-</sup> and a negative response to H<sub>2</sub>PO<sub>4</sub><sup>-</sup> (Figure 16).

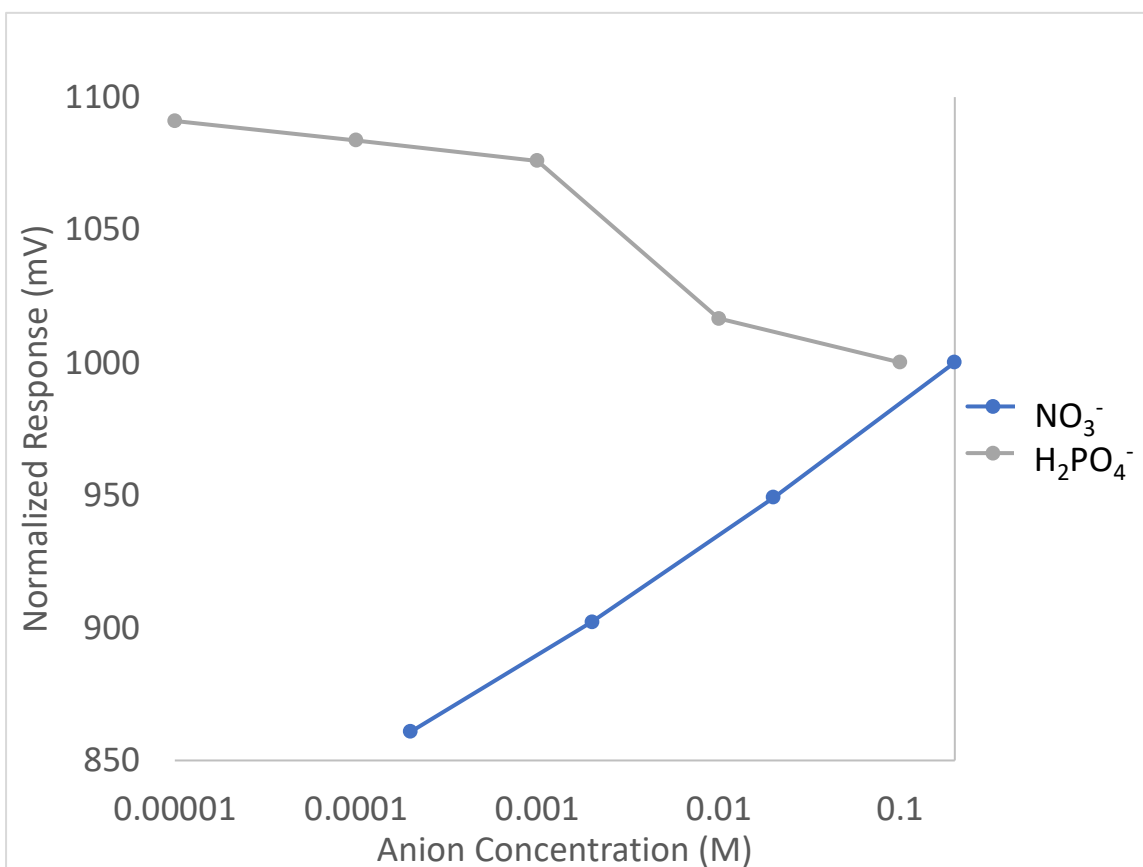
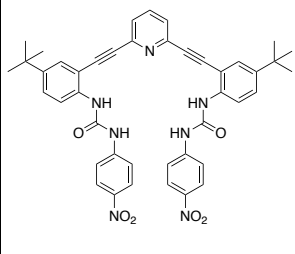


Figure 16. NBR, Pyridinium Core, Nitro Shoes.

Core:	Pyridine	Detection Limits (mM):	Sensitivity (mV/decade):			
Elbows:	t-butyl				$\text{NO}_3^-$ : 2.9	$\text{NO}_3^-$ : 47
Shoes:	Nitro					

ChemFETs were coated with NBR membrane containing TOAN and receptor. The receptor used had a pyridine core, t-butyl elbows and nitro shoes. The ChemFETs were tested for response to  $\text{NO}_3^-$ . In these experiments we observed a positive response to  $\text{NO}_3^-$  (Figure 17).

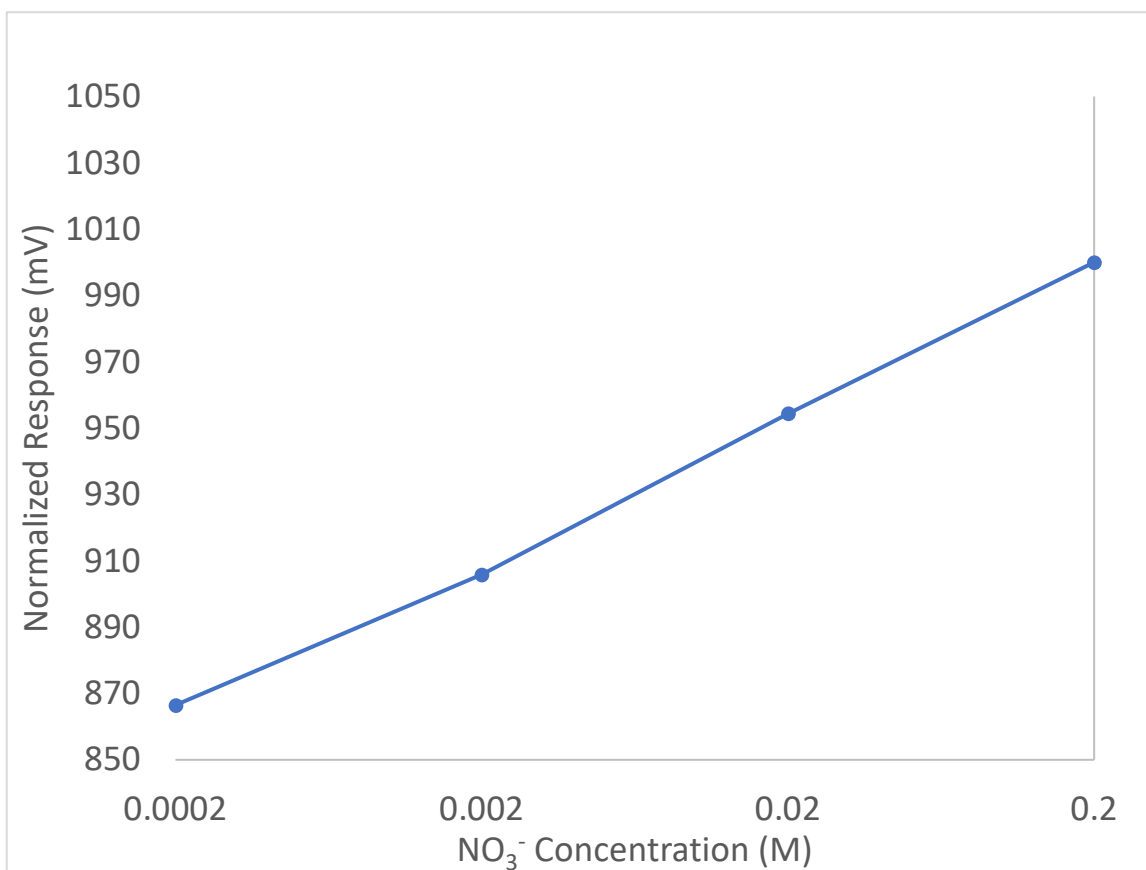


Figure 17. NBR, Pyridine Core, Nitro Shoes.

**Core Protonation State.** We hypothesized that if there was aqueous anion mobility through the polymer membrane, the protonation state of the pyridine and pyridinium cores would likely change with pH of the aqueous solution the sensor was submerged in. Additionally, a receptor with positive charge could potentially provide more cationic nature to the membrane, facilitating anion mobility in a similar manner to the ionic additive TOAN. The polymer formulations containing pyridine core receptors were used with the intent to evaluate any difference between pyridine and pyridinium core receptors; all other functional groups being the same (t-butyl elbows and nitro shoes). An examination of both structures indicate substantially different behavior should be expected if the protonation states remained distinct. The pyridinium core receptor contained five hydrogen-bonding donors in the pocket (pyridinium N-H, and all four urea N-H), while the pyridine core receptor contained only four hydrogen-bonding donors (the 4 urea N-H) and one hydrogen bonding acceptor (the pyridine N lone electron pair). Of note is that, while the exact  $pK_a$  of pyridine and pyridinium core scaffolds are not known, evaluations of similar scaffolds suggest a more acidic proton than pyridinium with a  $pK_a$  less than 5.<sup>14</sup> The nitrate series was measured to have pH ranging from ~6.6-7.3 depending on concentration. This would suggest if the aqueous environment influenced the protonation state of the receptors, both pyridine and pyridinium cores would equilibrate to the pyridine form.



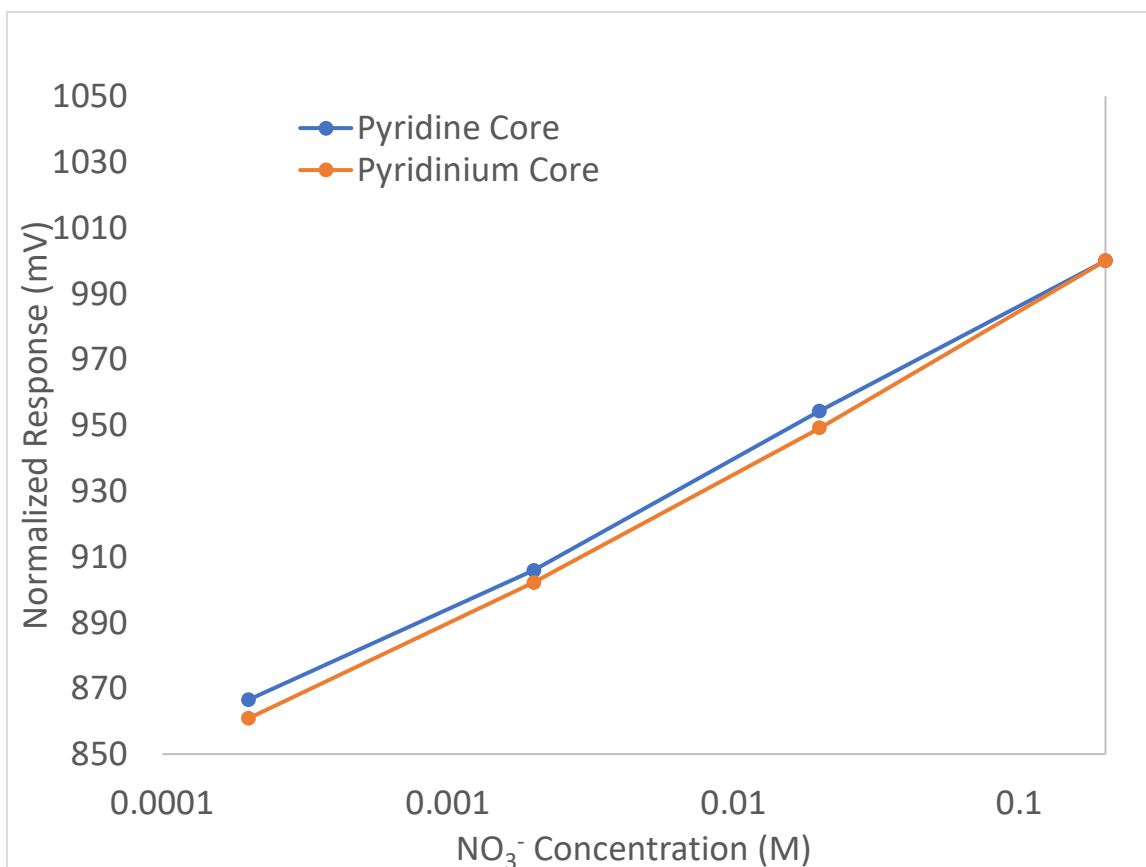
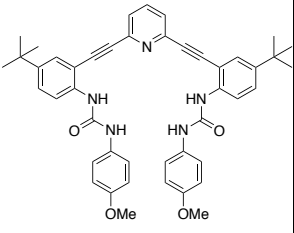


Figure 18. Core Protonation State Comparison.

ChemFETs containing pyridine receptors and ChemFETs containing pyridinium receptors were tested for response to NO<sub>3</sub><sup>-</sup>. Both displayed a virtually identical positive responses (Figure 18).

Core:	Pyridine	Detection Limits (mM): NO <sub>3</sub> <sup>-</sup> : 2.9 HPO <sub>4</sub> <sup>2-</sup> : 0.50 H <sub>2</sub> PO <sub>4</sub> <sup>-</sup> : 2.4	Sensitivity (mV/decade): NO <sub>3</sub> <sup>-</sup> : 47 HPO <sub>4</sub> <sup>2-</sup> : 24 H <sub>2</sub> PO <sub>4</sub> <sup>-</sup> : -31	
Elbows:	t-butyl			
Shoes:	Methoxy			

ChemFETs were coated with NBR membrane containing TOAN and receptor. The receptor used had a pyridine core, t-butyl elbows and methoxy shoes. The ChemFETs were tested for response to NO<sub>3</sub><sup>-</sup>, HPO<sub>4</sub><sup>2-</sup>, and H<sub>2</sub>PO<sub>4</sub><sup>-</sup>. In these experiments we observed a positive response to NO<sub>3</sub><sup>-</sup> and HPO<sub>4</sub><sup>2-</sup>, and a negative response to H<sub>2</sub>PO<sub>4</sub><sup>-</sup> (Figure 19)

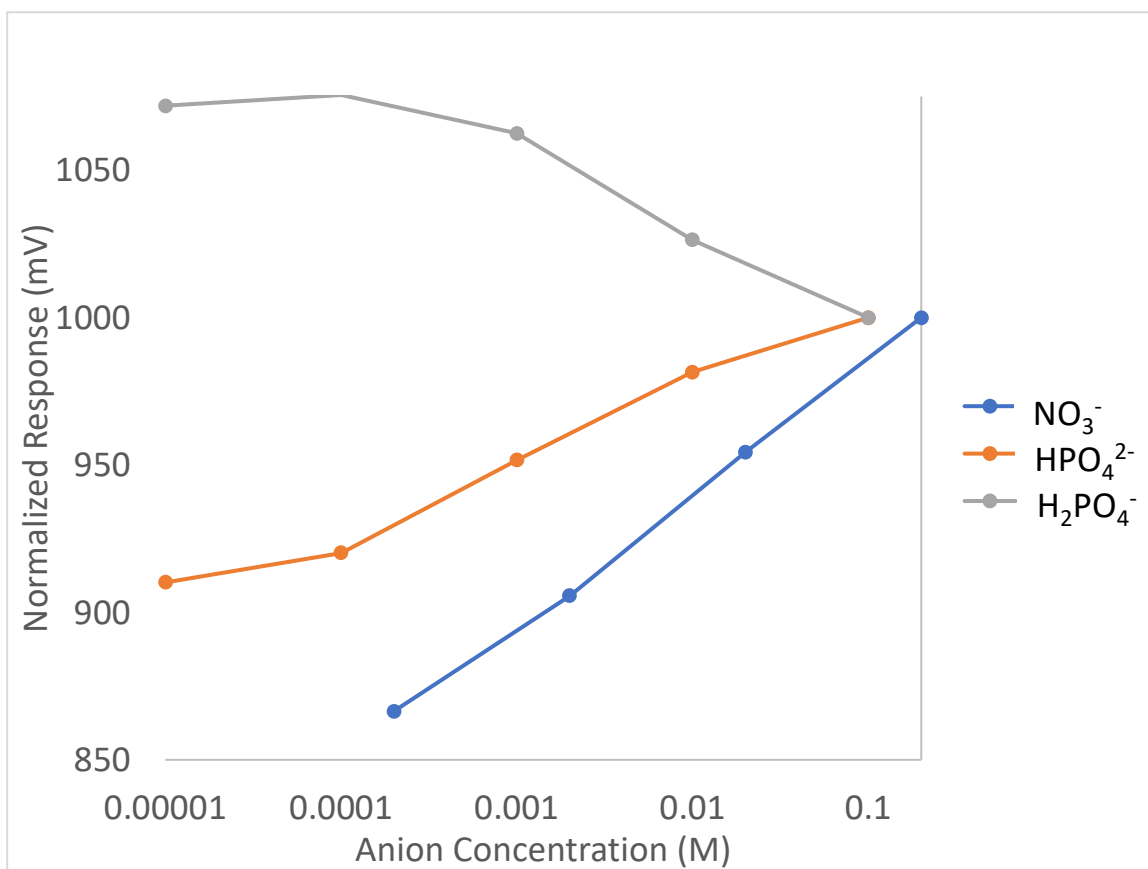
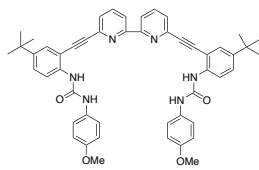


Figure 19. NBR, Pyridine Core, Methoxy Shoes.

Core:	Bipyridine	Detection Limits (mM): NO <sub>3</sub> <sup>-</sup> : 3.0 HPO <sub>4</sub> <sup>2-</sup> : 0.41 H <sub>2</sub> PO <sub>4</sub> <sup>-</sup> : 2.5 HSO <sub>4</sub> <sup>-</sup> : 2.2	Sensitivity (mV/decade): NO <sub>3</sub> <sup>-</sup> : 50 HPO <sub>4</sub> <sup>2-</sup> : 33 H <sub>2</sub> PO <sub>4</sub> <sup>-</sup> : -17 HSO <sub>4</sub> <sup>-</sup> : 44	
Elbows:	t-butyl			
Shoes:	Methoxy			

ChemFETs were coated with NBR membrane containing TOAN and receptor. The receptor used had a bipyridine core, t-butyl elbows and methoxy shoes. The ChemFETs were tested for response to NO<sub>3</sub><sup>-</sup>, HPO<sub>4</sub><sup>2-</sup>, H<sub>2</sub>PO<sub>4</sub><sup>-</sup>, and HSO<sub>4</sub><sup>-</sup>. In these experiments we observed a positive response to NO<sub>3</sub><sup>-</sup>, HPO<sub>4</sub><sup>2-</sup> and HSO<sub>4</sub><sup>-</sup>, and a negative response to H<sub>2</sub>PO<sub>4</sub><sup>-</sup> (Figure 20). The use of a bipyridine core represented one of the most extensive changes to the UO receptor motif. Instead of the standard pyridine core, a bipyridine core facilitated a larger binding pocket in order accommodate larger anions or twist the

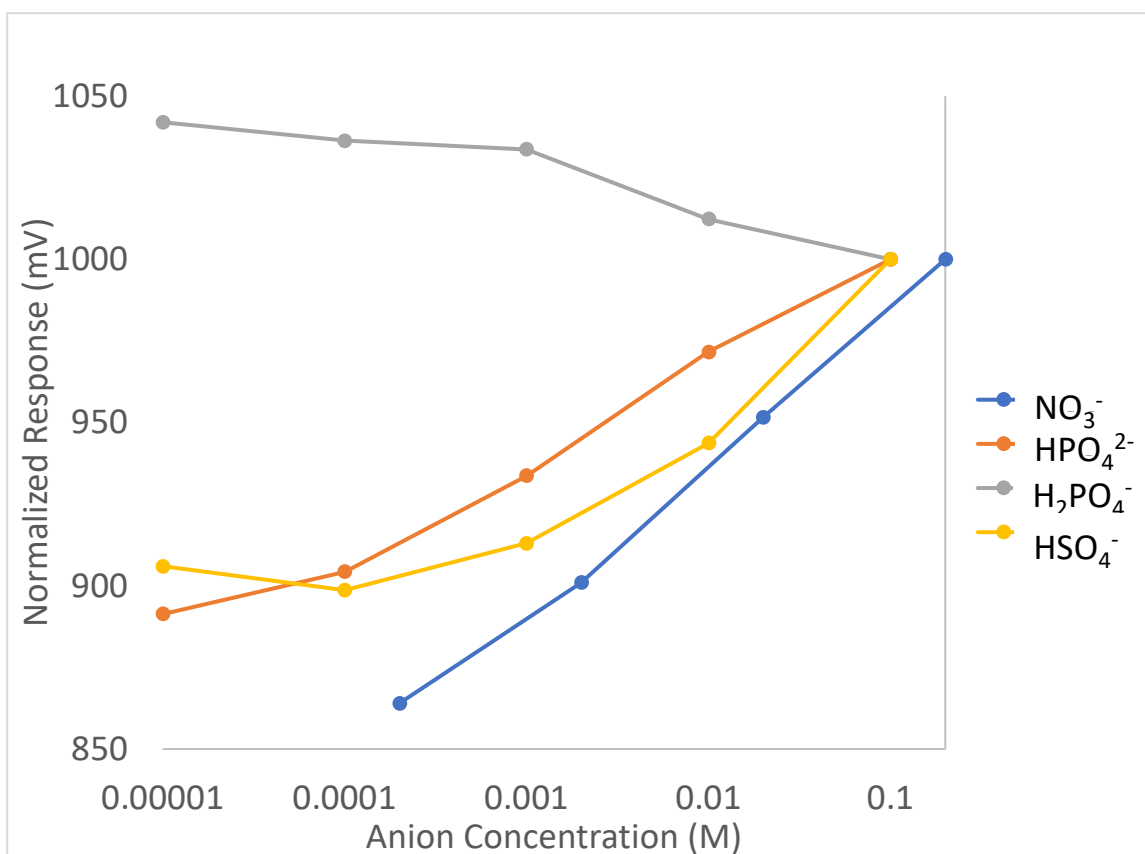


Figure 20. NBR, Bipyridine Core, Methoxy Shoes.

scaffold around to create a 2:1 (guest:host) binding ratio of two anions bound per receptor.

Core:	N/A	Detection Limits (mM): NO <sub>3</sub> <sup>-</sup> : 2.7 HPO <sub>4</sub> <sup>2-</sup> : 0.91 H <sub>2</sub> PO <sub>4</sub> <sup>-</sup> : 2.1	Sensitivity (mV/decade): NO <sub>3</sub> <sup>-</sup> : 46 HPO <sub>4</sub> <sup>2-</sup> : 30 H <sub>2</sub> PO <sub>4</sub> <sup>-</sup> : -25	N/A
Elbows:	N/A			
Shoes:	N/A			

Control ChemFETs were coated with NBR membrane containing TOAN but no receptor.

The ChemFETs were tested for response to NO<sub>3</sub><sup>-</sup>, HPO<sub>4</sub><sup>2-</sup>, and H<sub>2</sub>PO<sub>4</sub><sup>-</sup>. In these experiments we observed a positive response to NO<sub>3</sub><sup>-</sup> and HPO<sub>4</sub><sup>2-</sup>, and a negative response to H<sub>2</sub>PO<sub>4</sub><sup>-</sup>. (Figure 21).

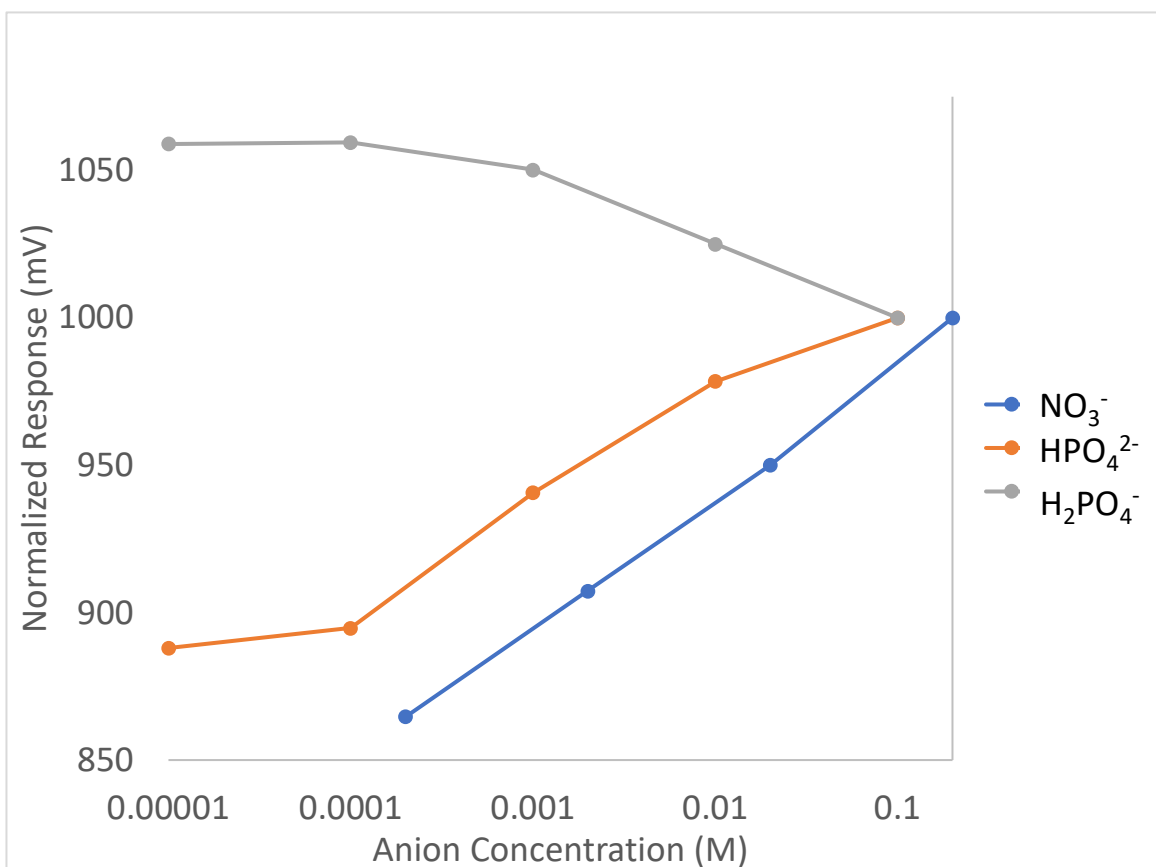
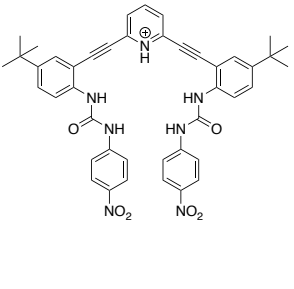


Figure 21. NBR, TOAN, No Receptor

**pH Sensitivity.** One practical concern to utilizing ChemFETs is potential pH sensitivity. Reinhoudt discussed applying a polyHEMA layer directly on the gate oxide to eliminate this pH sensitivity.<sup>9</sup> Our effort involved applying polyHEMA below the NBR. 650  $\mu$ l 3-(trimethoxysilyl)propyl methacrylate (MTPS) were added to a 50 ml round bottom flask along with 25 ml toluene along with 300  $\mu$ l DI water. The flask was fitted with a condenser. Three ChemFETs were fixed to a copper wire and suspended in the reaction solution. The ChemFETs were first cleaned by soaking in 30% H<sub>2</sub>O<sub>2</sub> for 20 minutes and then washed with DI water followed by ethanol. The flask was heated to 100°C and held there for 4 hours. The ChemFETs were then removed, washed with ethyl acetate then sonicated in ethyl acetate for 3 minutes. They were then rinsed once more with ethyl acetate and allowed to air dry.

The polyHEMA layer was then applied to the ChemFETs. First, 0.4g 2,2-dimethoxy-2-acetophenone (DMPA) was dissolved in 9.6g 2-hydroxyethyl methacrylate (HEMA). Approximately 2  $\mu$ l of this solution was placed on each ChemFET surface. These ChemFETs placed under N<sub>2</sub> atmosphere for 15 minutes. They were then cured by UV exposure for 5 minutes. The ChemFETs were then rinsed with ethyl acetate and then sonicated in ethyl acetate for 5 minutes. Lastly the ChemFETs were sonicated in ethanol for 5 minutes and then allowed to dry.

After the polyHEMA application the ChemFETs were coated with an NBR membrane containing TOAN and receptor, and run in comparison to control ChemFETs (identical in makeup, without the polyHEMA layer).

Core:	Pyridinium	Detection Limits (mM):	Sensitivity (mV/decade):			
Elbows:	t-butyl				(PolyHEMA) NO <sub>3</sub> <sup>-</sup> : 12	(PolyHEMA) NO <sub>3</sub> <sup>-</sup> : 22
Shoes:	Nitro				(No PolyHEMA) NO <sub>3</sub> <sup>-</sup> : 13	(No PolyHEMA) NO <sub>3</sub> <sup>-</sup> : 46

The receptor used had a pyridinium core, t-butyl elbows and nitro shoes. The ChemFETs were tested for response to NO<sub>3</sub><sup>-</sup> and to changes in pH. In these experiments we observed a positive response to both NO<sub>3</sub><sup>-</sup> and pH. Results showed that the polyHEMA layer reduced NO<sub>3</sub><sup>-</sup> sensitivity (Figure 22). The polyHEMA layer also made the ChemFETs nearly impossible to recycle.

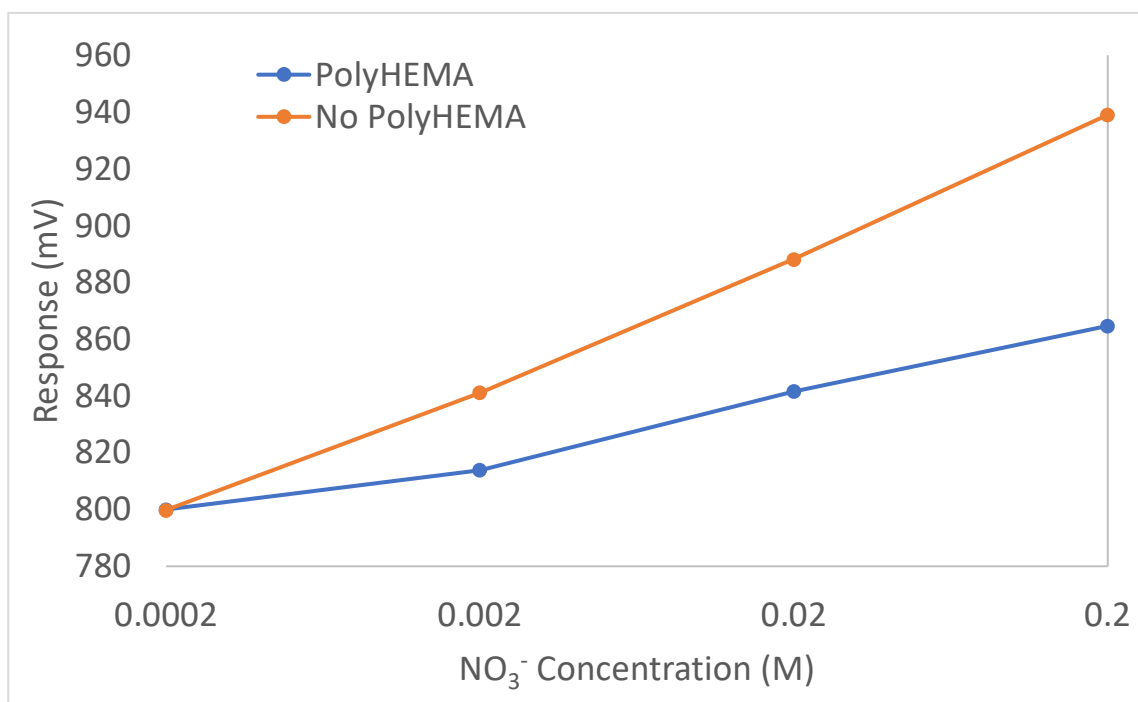


Figure 22. PolyHEMA Nitrate Sensitivity Comparison.

ChemFETs with both NBR and NBR with polyHEMA underlayer demonstrated pH sensitivity. We observed a slope of 25 testing ChemFETs with NBR only, and a slope of 10 testing ChemFETs with NBR and polyHEMA. Results showed that the polyHEMA layer reduced pH sensitivity as intended (Figure 23).

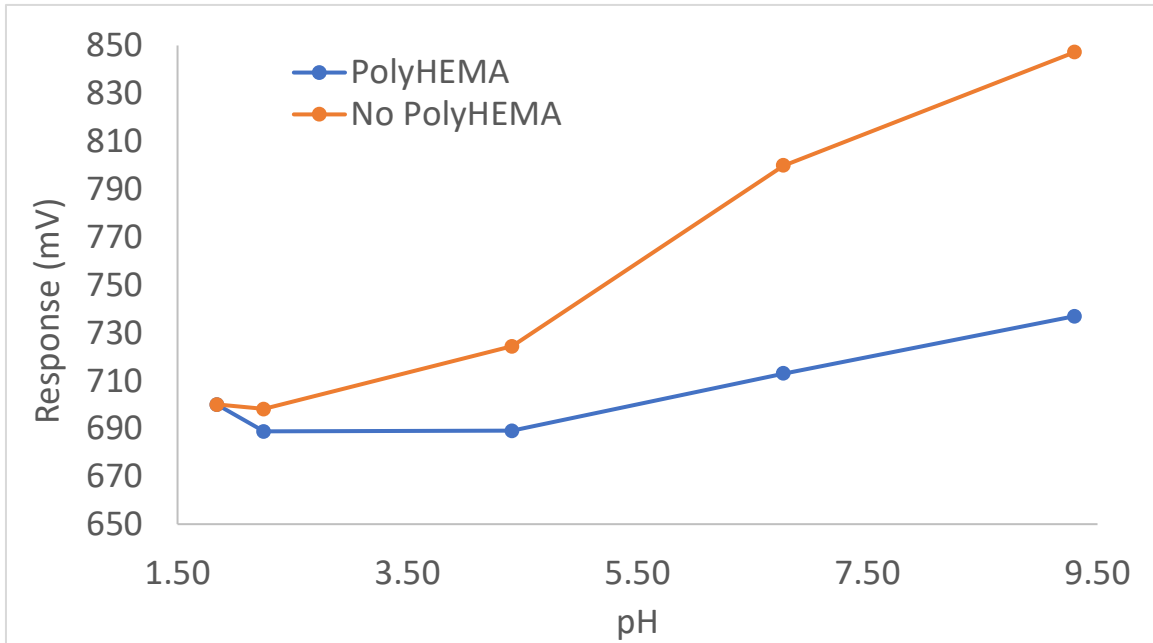


Figure 23. PolyHEMA pH Sensitivity Comparison.

Two different  $\text{HPO}_4^{2-}$  receptors from Valerie Pierre's lab at the University of Minnesota were evaluated. Four ChemFETs were coated with NBR membrane containing TREN.IAM receptor, and four ChemFETs were coated NBR membrane containing TREN.MAM receptor.<sup>13</sup> The ChemFETs were tested

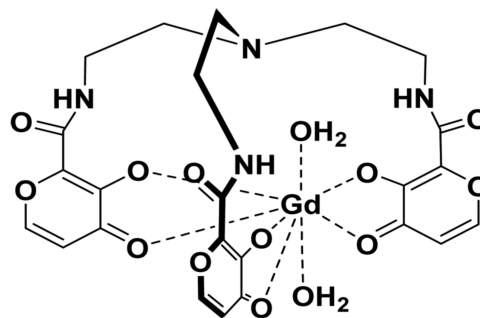


Figure 24. TREN.MAM Receptor

for response to  $\text{HPO}_4^{2-}$ . In these experiments we observed no significant response to  $\text{HPO}_4^{2-}$  (Figure 25).

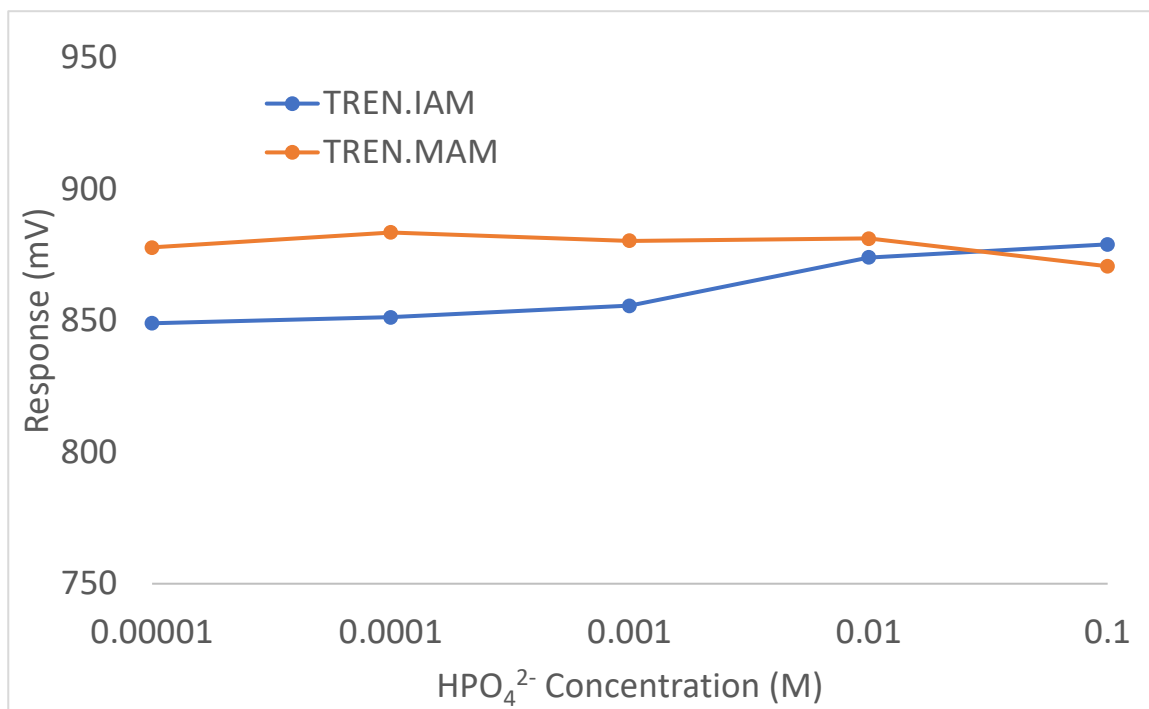


Figure 25. TREN.MAM and TREN.IAM in Hydrogen Phosphate.



**Polyvinyl Chloride Membranes.** We wanted an alternative gate oxide membrane to NBR. Other groups have observed that certain polymers actually affected the response to different analytes/targets. Therefore, we wanted another polymer system

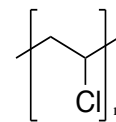


Figure 24. Polyvinyl Chloride (PVC).

in our toolkit. High molecular weight PVC (Figure 26) was obtained from Sigma Aldrich, and utilizing a readily-available plasticizer referenced in literature, *ortho*-nitrophenyl octyl ether (NPOE) (Figure 27). There was no definitive guidance in literature about optimal plasticizer amount so a screening approach was used to qualitatively evaluate

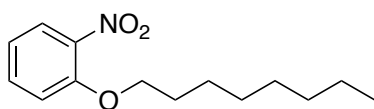


Figure 27. *ortho*-Nitrophenyl Octyl Ether (NPOE).

PVC with 65 wt. % plasticizer, 50 wt. % plasticizer, and 35 wt. % plasticizer, respectively. For example, a 50% plasticizer membrane containing both receptor and ionic additive would be still be 94.5% membrane (47.25 wt. % PVC and 47.25 wt. % NPOE), 0.5 wt. % receptor and 5 wt. % TOAN. For simplicity, the membranes are referred to as PVC 65-NPOE, PVC 50-NPOE, and PVC 35-NPOE.

By observation, the PVC 65-NPOE did not demonstrate suitable durability, and in fact fell off after the first week of evaluation. Four replicate samples confirmed this result. Further evaluations were conducted of PVC 50-NPOE and PVC 35-NPOE for sensor membrane suitability. Both performed satisfactorily over the first 10 runs, although PVC 50-NPOE eventually delaminated from the FET surface. Of note, the PVC 65-NPOE stock drop cast solution in anisole required no heating to dissolve, whereas the PVC 50-NPOE and PVC 35-NPOE drop cast solutions required heating to 80°C and

stirring for 1 hour in order to dissolve. The easy removal of PVC 50-NPOE prompted an evaluation of PVC 35-NPOE, which showed the most satisfactory performance.

**pH Testing.** The PVC/plasticizer membrane was also tested in a pH series to determine the pH sensitivity of the PVC membrane compared to the NBR membrane. Both ChemFETs with NBR and ChemFETs with NBR and polyHEMA underlayer demonstrated pH sensitivity, as described earlier in the chapter. We observed a slope of 25 testing ChemFETs with NBR, and a slope of 31 testing ChemFETs with PVC (Figure 28).

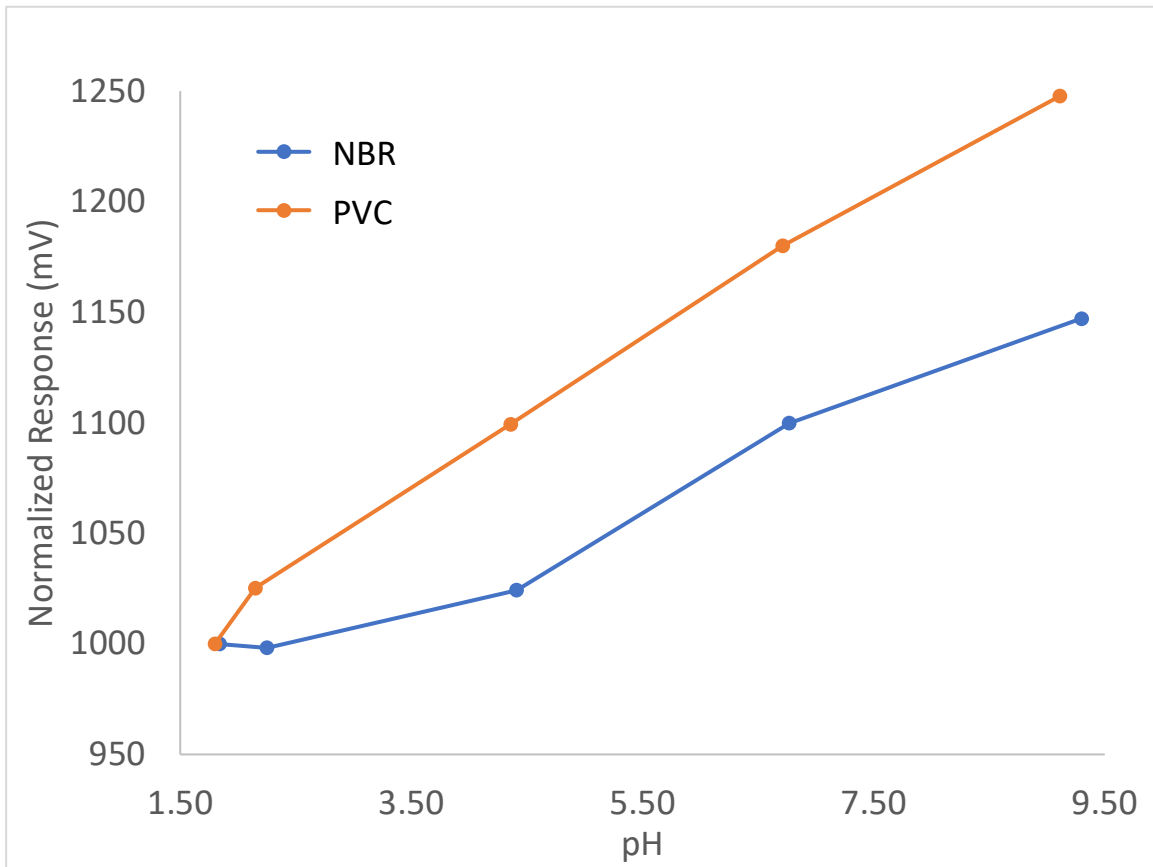
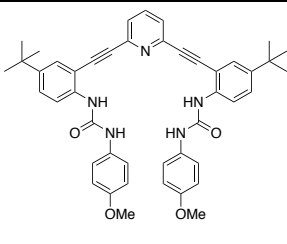


Figure 25. pH Testing of NBR vs PVC Membranes.

Core:	Pyridine	Detection Limits (mM): NO <sub>3</sub> <sup>-</sup> : 3.0 HPO <sub>4</sub> <sup>2-</sup> : 2.8 H <sub>2</sub> PO <sub>4</sub> <sup>-</sup> : 0.78 HSO <sub>4</sub> <sup>-</sup> : 30	Sensitivity (mV/decade): NO <sub>3</sub> <sup>-</sup> : 54 HPO <sub>4</sub> <sup>2-</sup> : 13 H <sub>2</sub> PO <sub>4</sub> <sup>-</sup> : -15 HSO <sub>4</sub> <sup>-</sup> : 33	
Elbows:	t-butyl			
Shoes:	Methoxy			

ChemFETs were coated with PVC 65-NPOE membrane containing TOAN and receptor.

The receptor used had a pyridine core, t-butyl elbows and methoxy shoes. The

ChemFETs were tested for response to NO<sub>3</sub><sup>-</sup>, HPO<sub>4</sub><sup>2-</sup>, H<sub>2</sub>PO<sub>4</sub><sup>-</sup>, and HSO<sub>4</sub><sup>-</sup>. In these

experiments we observed a positive response to NO<sub>3</sub><sup>-</sup>, HPO<sub>4</sub><sup>2-</sup> and HSO<sub>4</sub><sup>-</sup>, and a negative response to H<sub>2</sub>PO<sub>4</sub><sup>-</sup> (Figure 29).

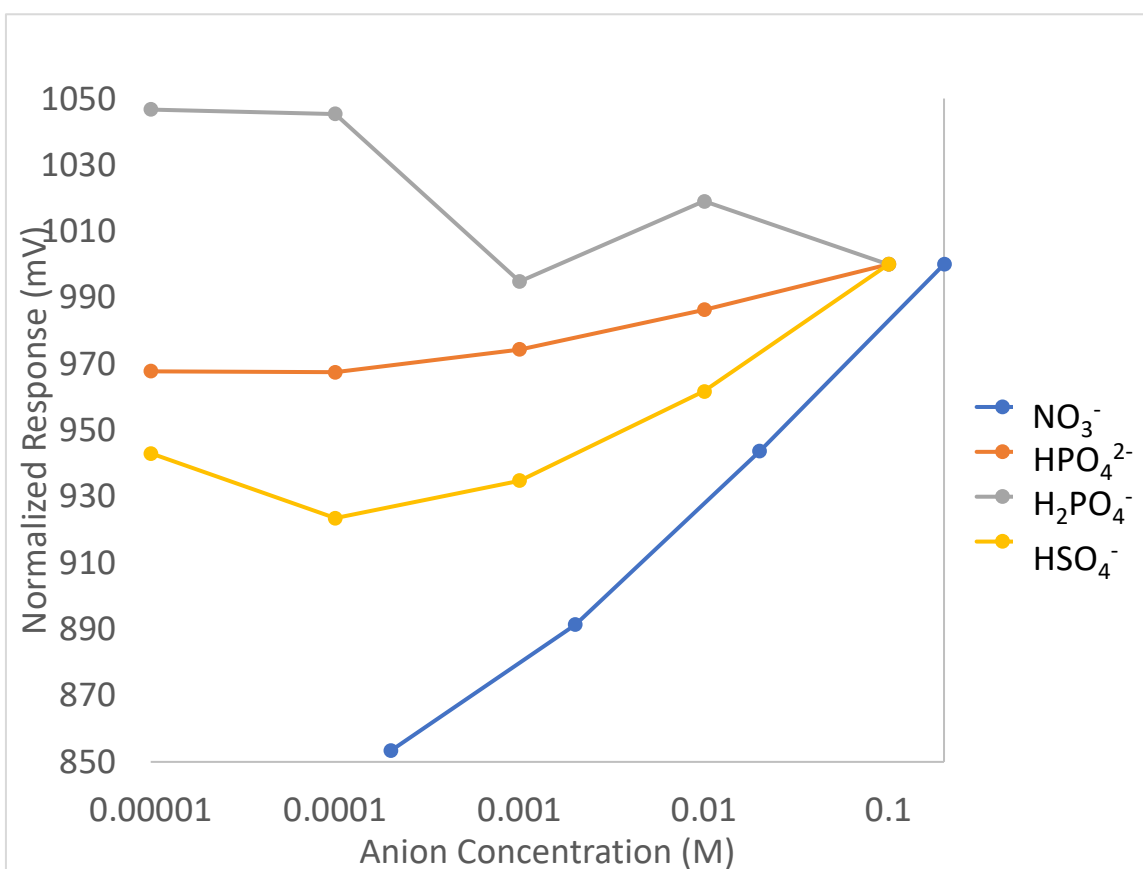
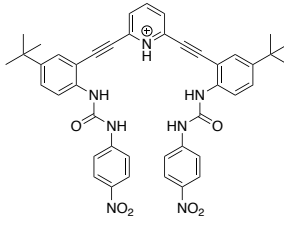


Figure 26. PVC 65-NPOE, Pyridine Core, Methoxy Shoes.

Core:	Pyridinium	Detection Limits (mM): NO <sub>3</sub> <sup>-</sup> : 3.0 HPO <sub>4</sub> <sup>2-</sup> : 3.3 H <sub>2</sub> PO <sub>4</sub> <sup>-</sup> : 1.3 HSO <sub>4</sub> <sup>-</sup> : 2.1	Sensitivity (mV/decade): NO <sub>3</sub> <sup>-</sup> : 41 HPO <sub>4</sub> <sup>2-</sup> : 14 H <sub>2</sub> PO <sub>4</sub> <sup>-</sup> : -4.0 HSO <sub>4</sub> <sup>-</sup> : 53	
Elbows:	t-butyl			
Shoes:	Nitro			

ChemFETs were coated with PVC 65-NPOE membrane containing TOAN and receptor.

The receptor used had a pyridinium core, t-butyl elbows and nitro shoes. The ChemFETs were tested for response to NO<sub>3</sub><sup>-</sup>, HPO<sub>4</sub><sup>2-</sup>, H<sub>2</sub>PO<sub>4</sub><sup>-</sup>, and HSO<sub>4</sub><sup>-</sup>. In these experiments we observed a positive response to NO<sub>3</sub><sup>-</sup>, HPO<sub>4</sub><sup>2-</sup> and HSO<sub>4</sub><sup>-</sup>, and a negative response to H<sub>2</sub>PO<sub>4</sub><sup>-</sup> (Figure 30).

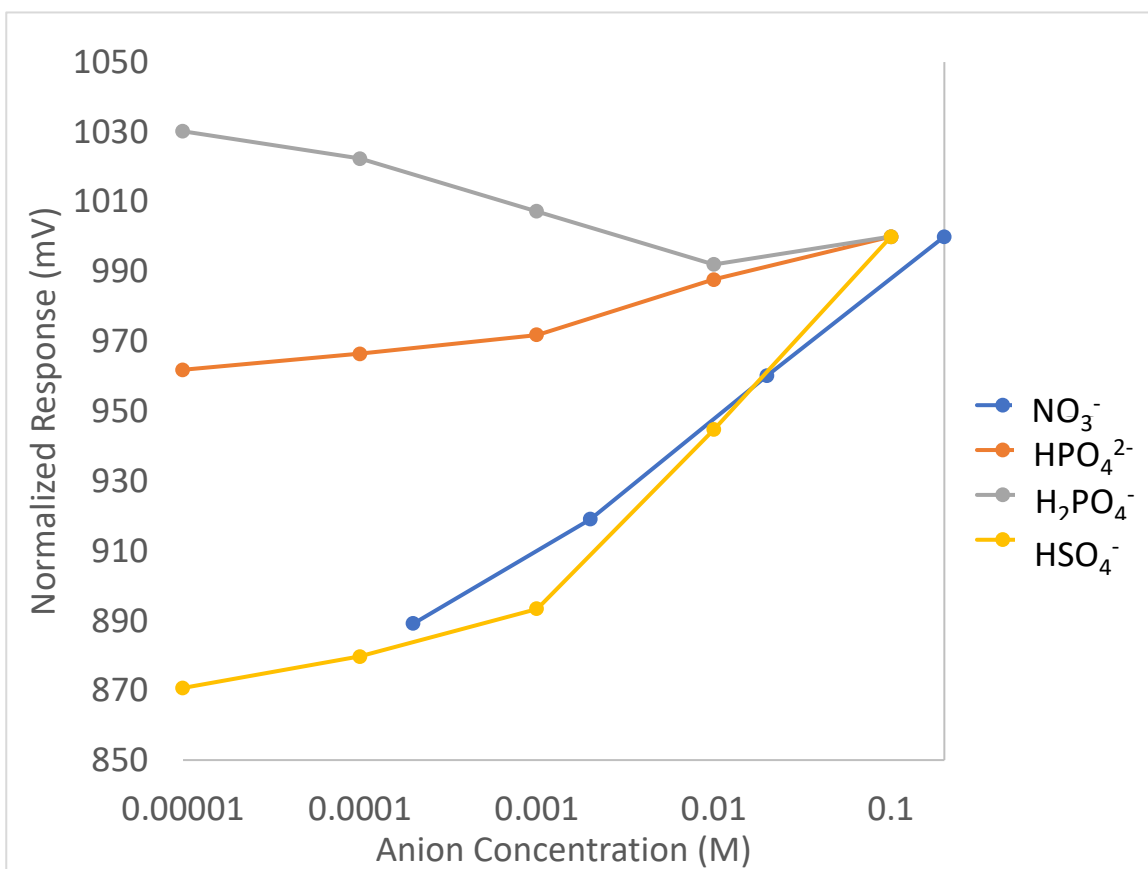
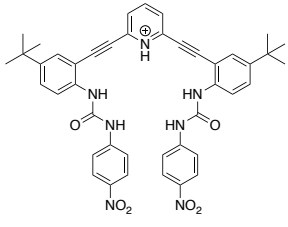


Figure 30. PVC 65-NPOE, Pyridinium Core, Nitro Shoes.

Core:	Pyridinium	Detection Limits (mM):	Sensitivity (mV/decade):	
Elbows:	t-butyl	NO <sub>3</sub> <sup>-</sup> : 3.0 HPO <sub>4</sub> <sup>2-</sup> : 1.3 H <sub>2</sub> PO <sub>4</sub> <sup>-</sup> : 1.5 HSO <sub>4</sub> <sup>-</sup> : 1.0	NO <sub>3</sub> <sup>-</sup> : 24 HPO <sub>4</sub> <sup>2-</sup> : 13 H <sub>2</sub> PO <sub>4</sub> <sup>-</sup> : -18 HSO <sub>4</sub> <sup>-</sup> : -11	
Shoes:	Nitro			

ChemFETs were coated with PVC 65-NPOE membrane containing 1/10 the standard amount of TOAN (0.5 wt % instead of 5 wt %) and receptor. The receptor used had a pyridinium core, t-butyl elbows and nitro shoes. The ChemFETs were tested for response to NO<sub>3</sub><sup>-</sup>, HPO<sub>4</sub><sup>2-</sup>, H<sub>2</sub>PO<sub>4</sub><sup>-</sup>, and HSO<sub>4</sub><sup>-</sup> in direct comparison to the previous experiment.

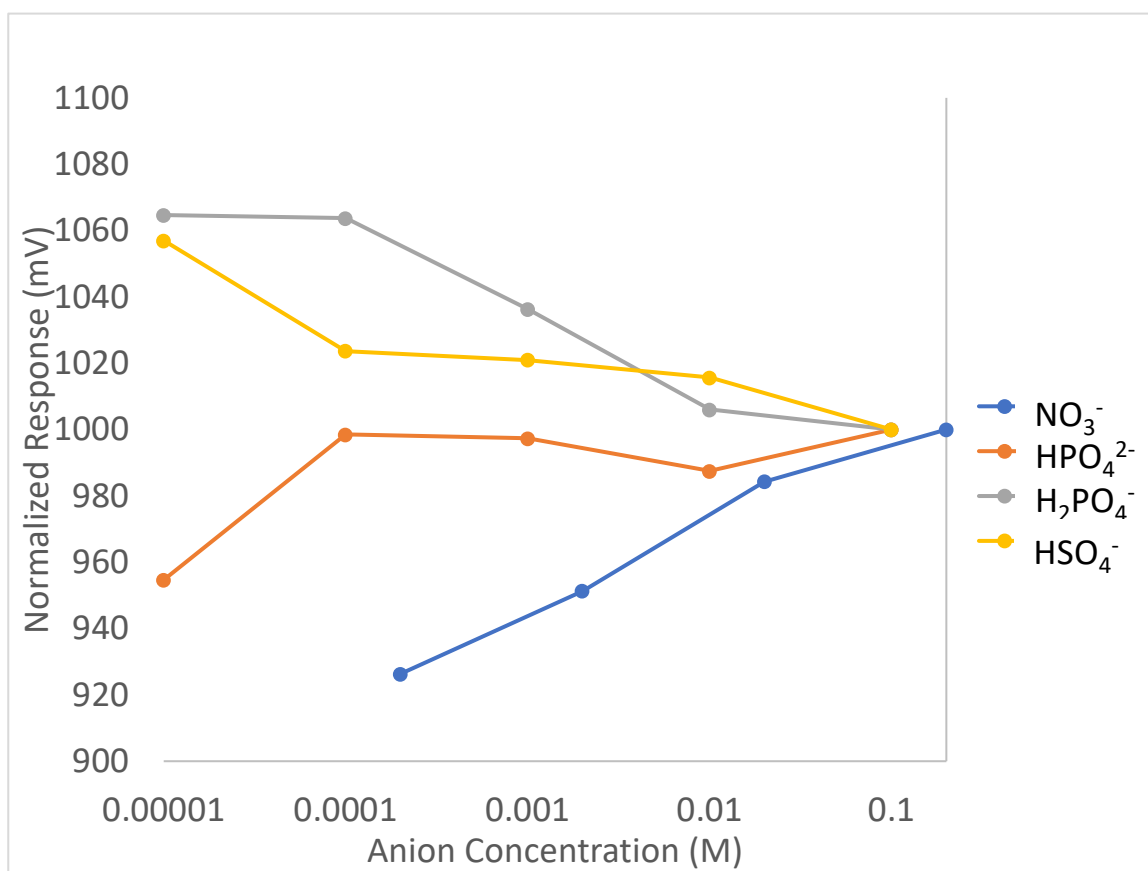


Figure 31. PVC 65-NPOE, Pyridinium Core, Nitro Shoes, 1/10 TOAN.

In these experiments we observed a positive response to NO<sub>3</sub><sup>-</sup>, HPO<sub>4</sub><sup>2-</sup> and HSO<sub>4</sub><sup>-</sup>, and a negative response to H<sub>2</sub>PO<sub>4</sub><sup>-</sup> (Figure 31). The shallower slopes of the responses indicated the effect of reducing TOAN by one order of magnitude.

Core:	N/A	Detection Limits (mM): NO <sub>3</sub> <sup>-</sup> : 0.40 HPO <sub>4</sub> <sup>2-</sup> : 0.10 H <sub>2</sub> PO <sub>4</sub> <sup>-</sup> : 0.40 HSO <sub>4</sub> <sup>-</sup> : 2.5	Sensitivity (mV/decade): NO <sub>3</sub> <sup>-</sup> : 30 HPO <sub>4</sub> <sup>2-</sup> : 5 H <sub>2</sub> PO <sub>4</sub> <sup>-</sup> : -16 HSO <sub>4</sub> <sup>-</sup> : 38	N/A
Elbows:	N/A			
Shoes:	N/A			

ChemFETs were coated with PVC 65-NPOE membrane containing TOAN only. The ChemFETs were tested for response to NO<sub>3</sub><sup>-</sup>, HPO<sub>4</sub><sup>2-</sup>, H<sub>2</sub>PO<sub>4</sub><sup>-</sup>, and HSO<sub>4</sub><sup>-</sup>. In these experiments we observed a positive response to NO<sub>3</sub><sup>-</sup>, HPO<sub>4</sub><sup>2-</sup> and HSO<sub>4</sub><sup>-</sup>, and a negative response to H<sub>2</sub>PO<sub>4</sub><sup>-</sup> (Figure 32).

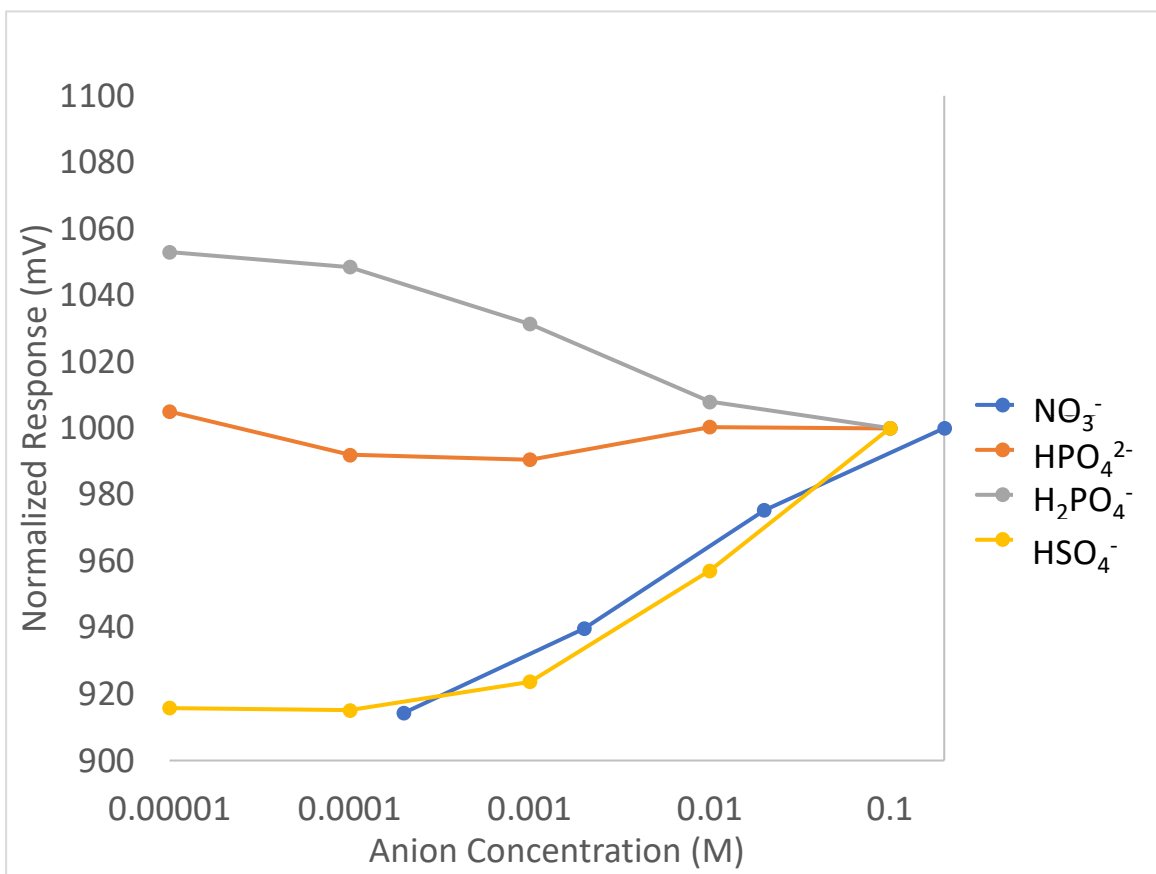
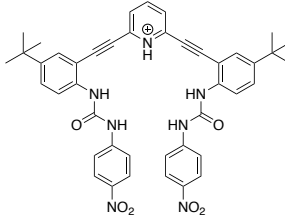


Figure 32. PVC 65-NPOE, TOAN, No Receptor.

Slightly shallower slopes indicate little effect by removing receptor and incorporating TOAN-only in the membrane.

Core:	Pyridinium	Detection Limits (mM): NO <sub>3</sub> <sup>-</sup> : N/A	Sensitivity (mV/decade): NO <sub>3</sub> <sup>-</sup> : 2.0	
Elbows:	t-butyl			
Shoes:	Nitro			

ChemFETs were coated with PVC 50-NPOE membrane containing receptor only. The ChemFETs were tested for response to NO<sub>3</sub><sup>-</sup>. In these experiments we observed no response to NO<sub>3</sub><sup>-</sup>, validating the need to incorporate TOAN in order to make working sensors (Figure 33).

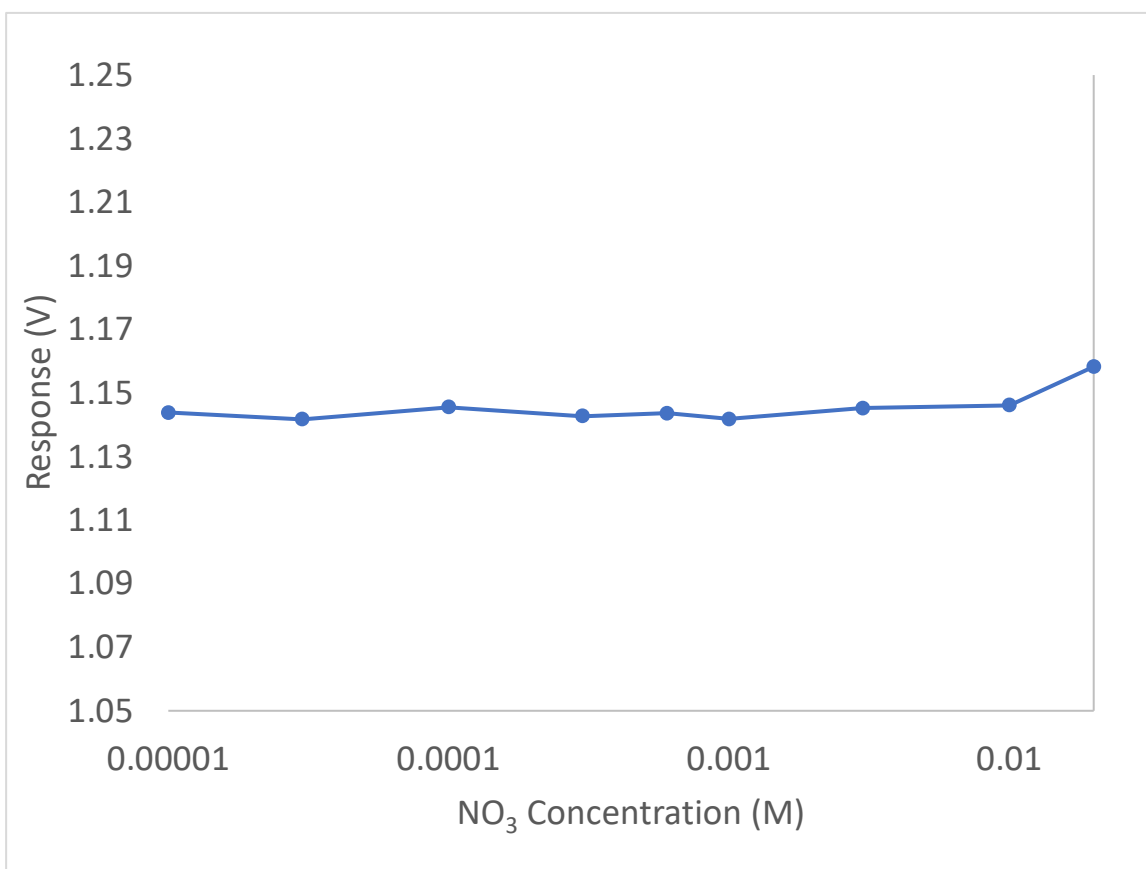
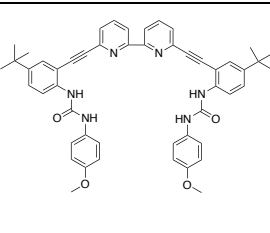


Figure 33. PVC 50-NPOE, Pyridinium Core, Nitro Shoes, No TOAN.

Core:	Bipyridine	Detection Limits (mM):	Sensitivity (mV/decade):	
Elbows:	t-butyl	NO <sub>3</sub> <sup>-</sup> : 3.5 HPO <sub>4</sub> <sup>2-</sup> : 1.5	NO <sub>3</sub> <sup>-</sup> : 36 HPO <sub>4</sub> <sup>2-</sup> : -7.0	
Shoes:	Methoxy	H <sub>2</sub> PO <sub>4</sub> <sup>-</sup> : 0.1 HSO <sub>4</sub> <sup>-</sup> : 1.6	H <sub>2</sub> PO <sub>4</sub> <sup>-</sup> : -6.5 HSO <sub>4</sub> <sup>-</sup> : 43	

ChemFETs were coated with PVC 50-NPOE membrane containing TOAN and receptor.

The receptor used had a bipyridine core, t-butyl elbows and methoxy shoes. The

ChemFETs were tested for response to NO<sub>3</sub><sup>-</sup>, HPO<sub>4</sub><sup>2-</sup>, H<sub>2</sub>PO<sub>4</sub><sup>-</sup>, and HSO<sub>4</sub><sup>-</sup>. In these

experiments we observed a positive response to NO<sub>3</sub><sup>-</sup> and HSO<sub>4</sub><sup>-</sup>, and a negative response to HPO<sub>4</sub><sup>2-</sup> and H<sub>2</sub>PO<sub>4</sub><sup>-</sup> (Figure 34).

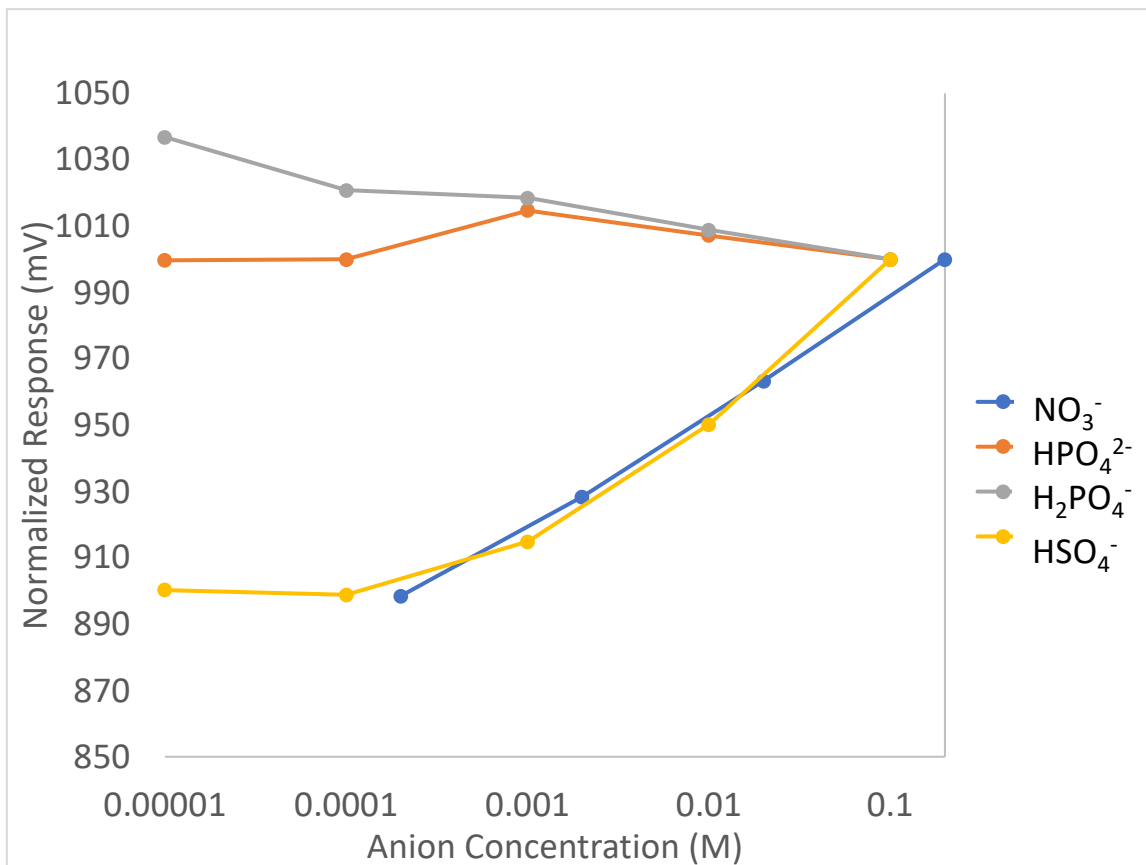
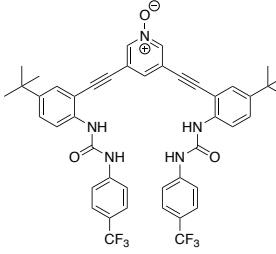


Figure 34. PVC 50-NPOE, Bipyridine Core, Methoxy Shoes.



Core:	N-confused N-oxide	Detection Limits (mM):	Sensitivity (mV/decade):			
Elbows:	t-butyl				NO <sub>3</sub> <sup>-</sup> : 3.1	NO <sub>3</sub> <sup>-</sup> : 35
Shoes:	CF <sub>3</sub>				HPO <sub>4</sub> <sup>2-</sup> : 6.3	HPO <sub>4</sub> <sup>2-</sup> : 30
		H <sub>2</sub> PO <sub>4</sub> <sup>-</sup> : 0.30	H <sub>2</sub> PO <sub>4</sub> <sup>-</sup> : -45			
		HSO <sub>4</sub> <sup>-</sup> : 0.90	HSO <sub>4</sub> <sup>-</sup> : 43			

ChemFETs were coated with PVC 50-NPOE membrane containing TOAN and receptor.

The receptor used had an N-confused N-oxide pyridinium core (the term “N-confused” refers to a receptor with the pyridinium N outside the binding pocket), t-butyl elbows and CF<sub>3</sub> shoes. The ChemFETs were tested for response to NO<sub>3</sub><sup>-</sup>, HPO<sub>4</sub><sup>2-</sup>, H<sub>2</sub>PO<sub>4</sub><sup>-</sup>, and HSO<sub>4</sub><sup>-</sup>. In these experiments we observed a positive response to NO<sub>3</sub><sup>-</sup>, HPO<sub>4</sub><sup>2-</sup> and HSO<sub>4</sub><sup>-</sup>, and a negative response to H<sub>2</sub>PO<sub>4</sub><sup>-</sup> (Figure 35).

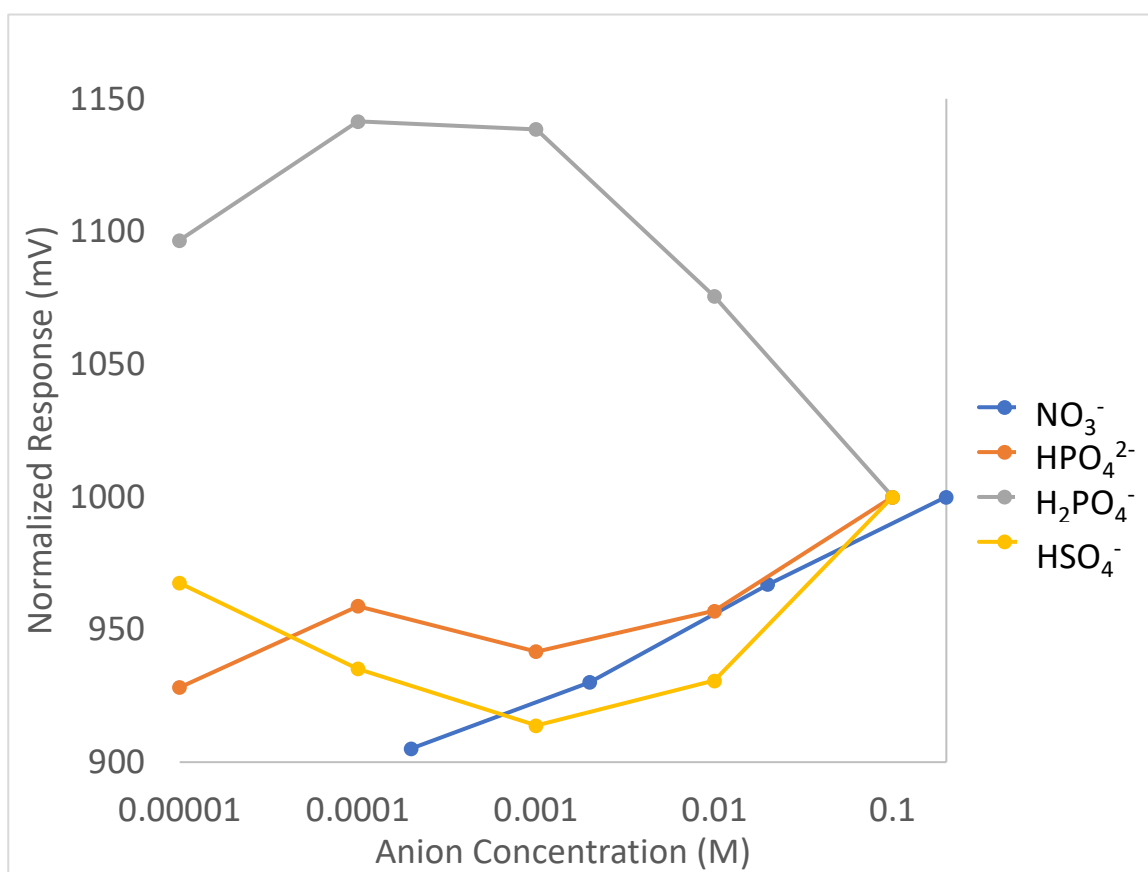


Figure 35. PVC 50-NPOE, N-Confused N-Oxide Core, CF<sub>3</sub> Shoes.

**Halogen-Bonding Receptors.** The halogen bonding receptor represented another large structural departure from the standard UO receptor scaffold. The entire bisurea and shoe pendant portions of the standard scaffold was replaced on each side by an iodine acting as a halogen bond donor (Figure 36).

The halogen bonding receptor with sulfone elbows had suspected affinity to  $\text{Cl}^-$  and  $\text{H}_2\text{PO}_4^-$  anions. Of

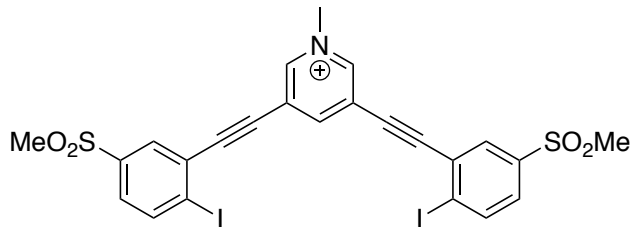
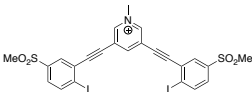


Figure 36. Halogen-Bonding Receptor.

particular interest of the halogen bonding receptors was the N-methylation of the pyridinium nitrogen, resulting in a permanently charged receptor (the term “permanent” being used to separate N-methylation from a protonated pyridinium core; where the latter loses the charge with pH of the aqueous solution, and the former does not).

Functional group differences in the halogen bonding receptor necessitated a departure from anisole as the solvent, as the halogen bonding receptor would not dissolve (even after application of heat, sonication, and stirring over 48 hrs). Acetonitrile, DMSO, acetone, ethanol, toluene, and THF were all evaluated. The criteria were that the new solvent must dissolve the receptor, PVC, and NPOE plasticizer. THF was the only solvent that successfully dissolved all three components. Initial studies were conducted on glass slides ensuring THF was a suitable drop cast medium. These simple studies comprised of drop casting five drops at 15-minute intervals, and observing the physical properties of the membrane that formed. After the qualitative observations that the THF drop cast solutions produced a suitable membrane, and that the THF evaporated within just a few minutes (compared to the 10+ minutes for anisole), THF was deemed an acceptable drop cast solvent and membranes were prepared via drop cast from THF.

Core:	N-confused N-methyl	Detection Limits (mM):	Sensitivity (mV/decade):		
Elbows:	Sulfone		Cl <sup>-</sup> : 4.0		Cl <sup>-</sup> : 80
Shoes:	Iodide		Without top pt: Cl <sup>-</sup> : 5.0		Without top pt: Cl <sup>-</sup> : 39

To evaluate the performance of the halogen bonding receptor as a replacement for both receptor and ionic additive, a drop cast solution was made with only the halogen bonding receptor (no TOAN), and PVC 35-NPOE membrane. This was then compared with control blanks, which were also drop casted from THF. Results in Cl<sup>-</sup> were very promising, with a positive slope observed for ChemFETs with receptor, in contrast to ChemFETs without (Figure 37). However, the response at the highest concentration seemed to be anomalously high, producing a slope between the top two points higher than the theoretical maximum of 59 mV/decade described by the Nernst equation.<sup>12</sup>

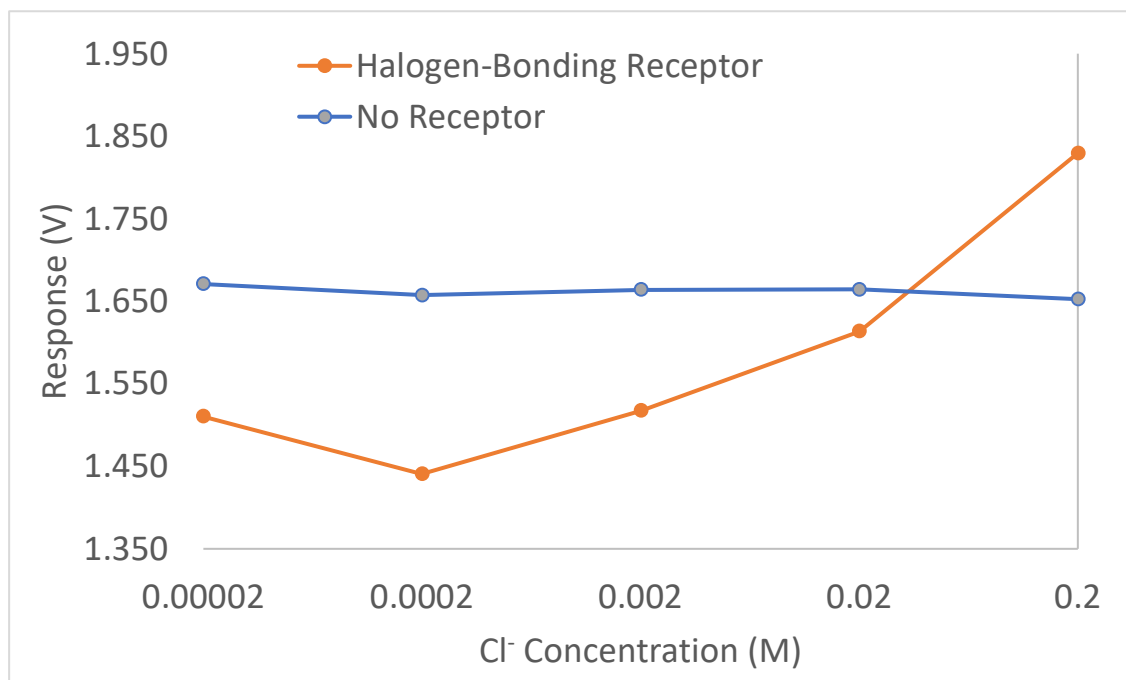
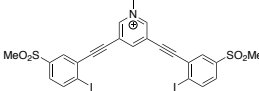


Figure 37. Halogen-Bonding Receptor in Chloride.

Results are reported for the raw data, as well as the data if the top point was removed as anomalous.

Comparison of halogen-bonding receptor with blank ChemFETs (PVC and plasticizer only – no receptor or TOAN), shows a significant difference between the halogen bonding receptor-embedded sensors and the blank control sensors.

Core:	N-confused N-methyl	Detection Limits (mM):	Sensitivity (mV/decade):			
Elbows:	Sulfone				NO <sub>3</sub> <sup>-</sup> : 1.4	NO <sub>3</sub> <sup>-</sup> : 21
Shoes:	Iodide					

The same set of halogen-bonding and blank sensors were tested for response to NO<sub>3</sub><sup>-</sup>. In these experiments we observed a positive response to NO<sub>3</sub><sup>-</sup> from ChemFETs with receptor (Figure 38).

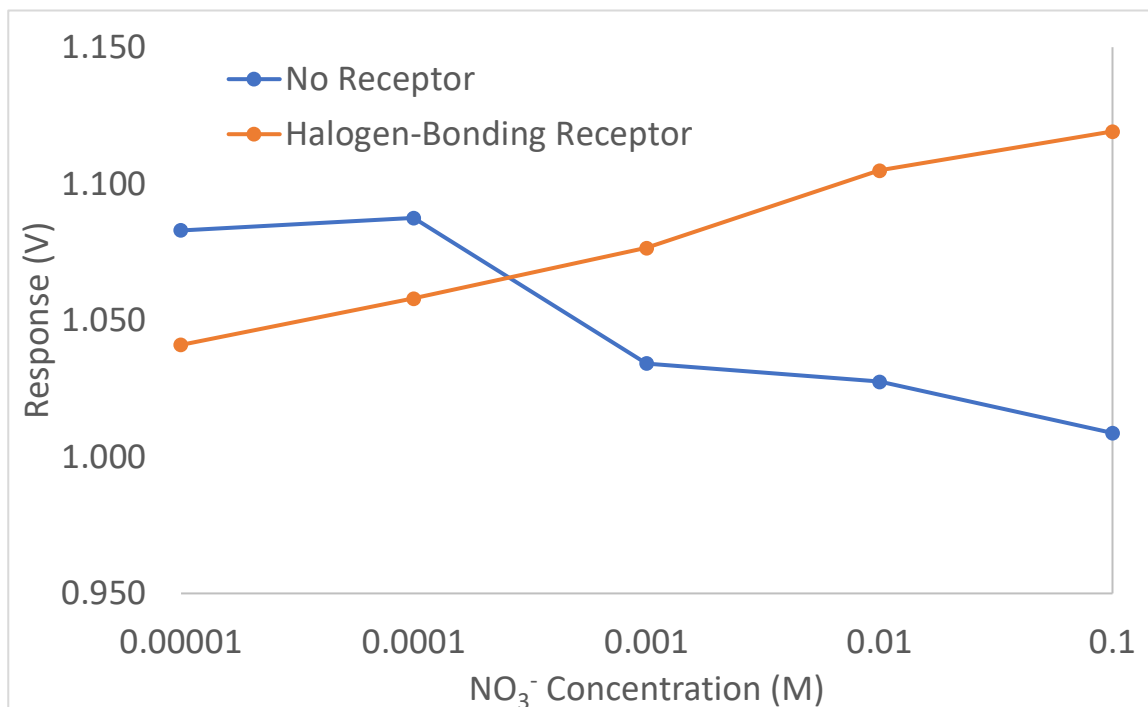


Figure 38. Halogen-Bonding Receptor in Nitrate.

Sensor results in Cl<sup>-</sup> and NO<sub>3</sub><sup>-</sup> provided an early indication that the permanently charged halogen-bonding receptors worked in the absence of any ionic additives. To date this was

the first successful ChemFET the DWJ lab had made without the use of TOAN or another ionic additive. The successful performance of this lends credence to further investigation of charged receptors.

**Longevity and Storage.** An evaluation of storage condition and effect on ChemFETs was evaluated. Initially FETs were stored in 0.5M analyte solutions based on recommendations from literature, but we had concerns that in our particular setup this was negatively impacting longevity.<sup>7</sup> This was not observed to be a problem with sensors stored in  $\text{NO}_3^-$ , but sensors stored in  $\text{H}_2\text{PO}_4^-$  were being destroyed by the phosphate. Storing the sensors dry was an initial approach to addressing this problem, but one of the key factors we took into consideration for wet vs dry storage was equilibration time. A major concern was that if the sensors were stored dry, they would take an inordinate

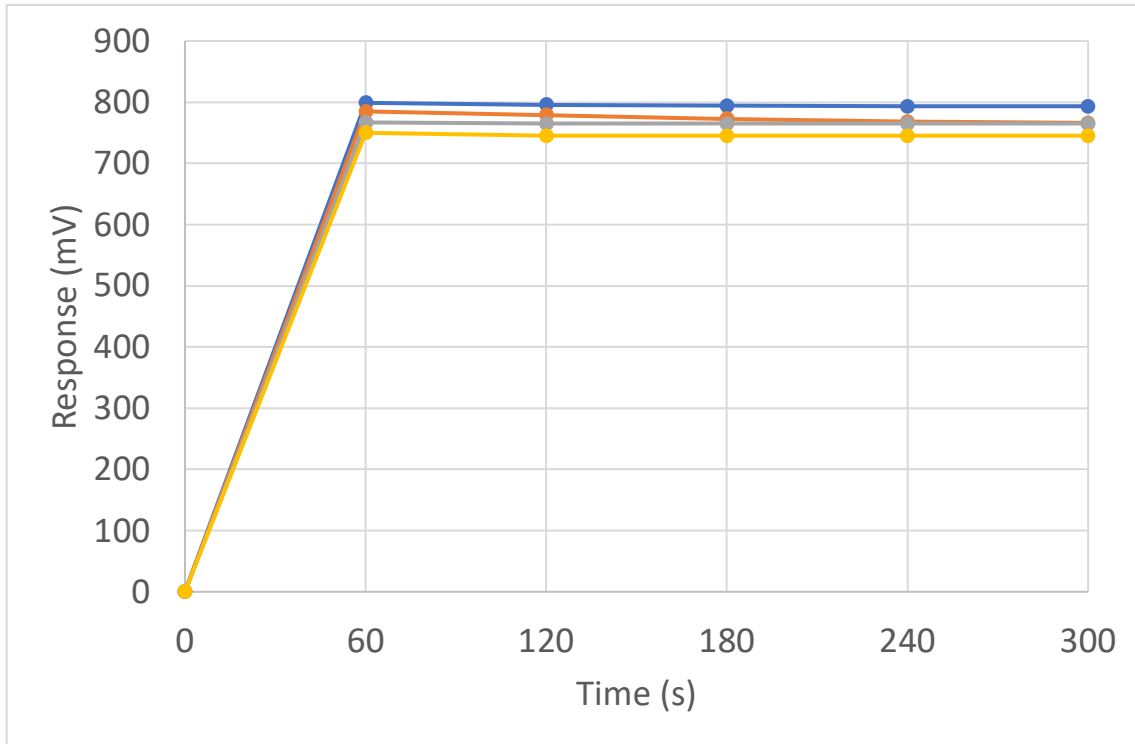


Figure 39. Equilibration Curves for Wet ChemFET Storage. Readings were taken every 60 seconds for the entire 5-minute period of a run. The four curves represent readings from each of four sensors.

amount of time to reach equilibrium. Figure 39 plots equilibration curves for  $\text{NO}_3^-$  storage, demonstrating how quickly the sensors reached their equilibrium reading. We then conducted an evaluation of dry storage of FETs in order to determine if the sensors were able to come to equilibrium in a reasonable amount of time. Figure 40 demonstrated that sensors under dry storage still came to equilibrium time in well under 5

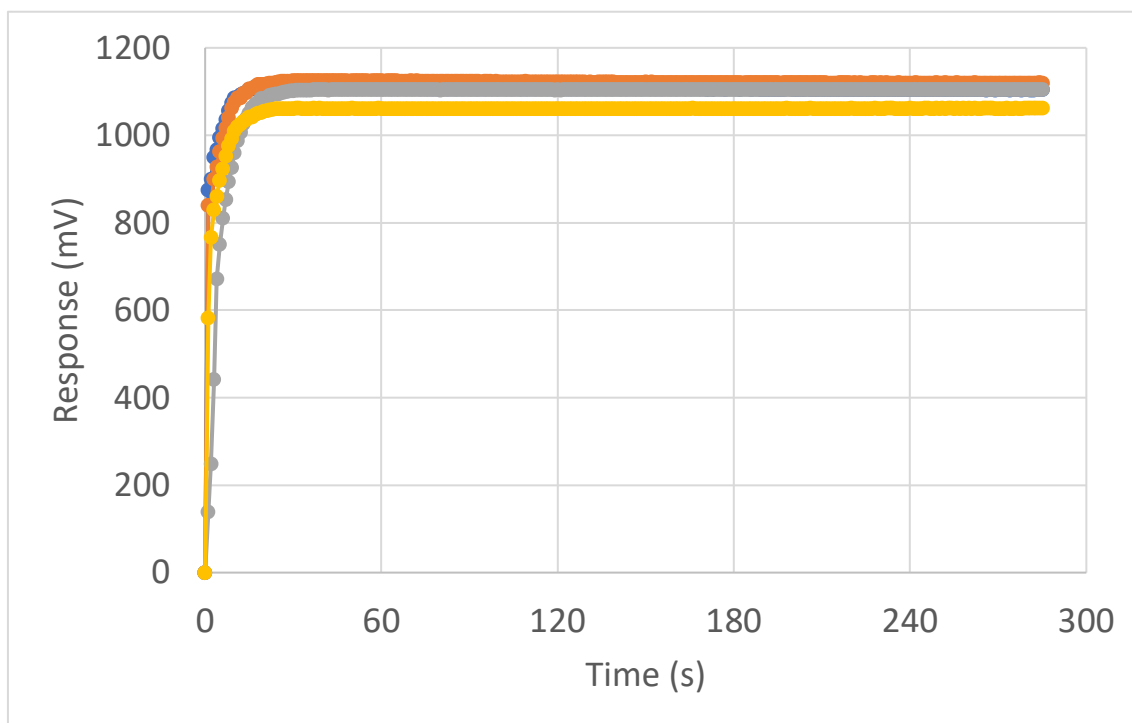


Figure 40. Equilibration Curves for Dry ChemFET Storage. Readings were taken every second for the entire 5-minute period of a run. The four curves represent readings from each of four sensors.

minutes (which was the standard length of each ChemFET run data point). The evaluation included a 30-minute soak in 0.2M  $\text{NO}_3^-$  prior to the test runs. The success of the dry storage evaluation made dry storage of ChemFETs standard. Prior to any evaluation dry-storage ChemFETs were soaked for 30 minutes in the highest concentration solution that would be tested, prior to any test runs. Of note is that the ChemFET setup changed between wet and dry storage evaluations; the wet storage system recorded a response every 60 seconds out to the end of the five-minute run, while

the dry storage system recorded a response every second for the entirety of the five-minute run. This explains the difference in appearance of the two equilibration graphs, however, the important detail remains clear and that is that the ChemFETs reached equilibrium response well within the five-minute sensing run time.

## CHAPTER IV: CONCLUSION AND FUTURE DIRECTION

**Conclusion.** ChemFETs can be successfully utilized to incorporate guest-host interaction to measure analyte concentration. We picked out off-the-shelf ChemFETs, polymers, deposition method and used an off-the-shelf nitrate receptor cocktail designed for ISEs along with another literature-derived formulation for an ammonium-sensing ChemFET and developed and validated a recyclable and high-throughput platform for testing different polymer membrane formulations. This was demonstrated to successfully measure total-N concentration with promising agricultural applications. Ordered selectivity coefficients were compared to the Hofmeister Series.

Several arylethynyl bisurea scaffold receptors were characterized by the ChemFET platform for affinity to a variety of common anions. A new gate oxide membrane was developed and successfully evaluated on ChemFETs. We evaluated the effect of the ionic additive TOAN, and demonstrated that uncharged receptors require ionic additive in order to function. The protonation state of pyridine and pyridinium cores was evaluated, and appeared to have identical performance suggesting the protonation state of pyridine and pyridinium cores change with solution pH. We evaluated a means of eliminating pH sensitivity using a polyHEMA layer between the gate oxide and analyte-sensitive membrane, and observed reduction in pH sensitivity as well as drawbacks of the method. An evaluation of charged receptors demonstrated a successful ChemFET device without any TOAN for the first time in the DWJ lab.



## **Future Direction.**

**Design of Experiments.** Tremendous potential exists for incorporating statistical analysis into ChemFET research. Design of experiments (DOE) utilizes statistical analysis and response surface design to analyze numerous system inputs for optimization. Numerous system conditions are input as independent variables, and then the results are analyzed in order to determine the relative influence of each. The computer modeling of the DOE program then produces an optimal design based on the desired dependent variable outcomes.

**Plasticizer.** The simplest application of DOE for ChemFETs would be to optimize the amount of NPOE plasticizer used in the PVC membrane. This would entail a simple 1-factor design with amount of plasticizer as the independent variable and several options for the dependent variable. One option for the dependent variable is to use sensitivity or slope, where maximizing slope is the optimization criteria. Another option is to use equilibration time, with shorter time being most optimal. Adhesion could also be used as it is an important factor relating to plasticizer amount, although this would potentially be a difficult factor to measure. Longevity (e.g. “remains adhered for 10 consecutive runs” or remains adhered for 3 months”) could potentially be used. Plasticizer amount has previously been shown to greatly impact longevity of the membrane on the FET surface, with 65% weight percent plasticizer not adhering long enough for a single run.

**Receptor and Ionic Additive.** A slightly more involved DOE analysis could use amounts of receptor and ionic additive (e.g. TOAN) as the independent variables. Maximizing sensitivity/slope as the dependent variable seems to be the most obvious

application for optimization, although the same data could be used to maximize such factors as equilibration time or selectivity.

**Structural DOE.** Structural optimization of receptors would be the most involved application of DOE, and would be quite synthesis-heavy. For independent variables, structural DOE would involve assigning numerical values to factors such as number of hydrogen bond donors and acceptors, cavity size, bite angle, and strengths of hydrogen-bond donors and acceptors. DOE could potentially output optimal designs, with a strong caveat that DOE is not chemical software and may in fact recommend receptor molecule designs not structurally or chemically possible. For this optimization FET-based measurements such as sensitivity or selectivity could be used as dependent variables. Additionally, factors such as binding constant, fluorescence, or others could be used as the dependent variable(s) depending on the goal of the study. However, structural DOE could also provide information on past experiments. Structural information could be entered on receptor molecules previously synthesized and characterized, results such as binding constants could be used to provide the DOE software input as to their performance, and then the software could then mathematically make a determination of the significance of each factor.

**Charged Receptors.** Positively-charged receptors certainly merit further investigation for anion sensing. Although this was briefly attempted when comparing pyridine and pyridinium-core receptors, the  $pK_a$  of the pyridinium was thought to render both the same protonation state when submerged in similar pH solutions. Therefore, further investigation into more permanently charged receptors seems to be in order. Receptors with a positive charge unaffected by pH would theoretically act in a similar manner to the

ionic additive TOAN, which was previously demonstrated to provide a suitable response even when it was the only component in the gate oxide membrane.

The first charged receptor meriting further investigation is the N-methyl-core variant of the classic UO receptor. Extensive studies have been conducted on the binding and fluorescence of this receptor with varying functionality in the “core,” “elbow,” and “shoe” locations on the scaffold. The additional functionality of the N-methylated variant represents a promising area of further research.

Numerous other UO receptor scaffolds with varying core, elbow, and shoe functionality have been synthesized by the DWJ and Haley labs anion sensing collaboration. Further studies are warranted, including evaluation in ChemFETs as well as providing additional functionality for a DOE evaluation.

**Soil Evaluation.** To evaluate more realistic usage of ChemFETs in agricultural applications, a total-N study could be conducted on soil samples containing known amounts of nitrates and ammonium, comparing ChemFET readings to the known amounts present in the control sample. This would provide a more realistic evaluation of ChemFETs in an agricultural application.

APPENDIX: CHAPTER II FIXED INTERFERENCE DATA

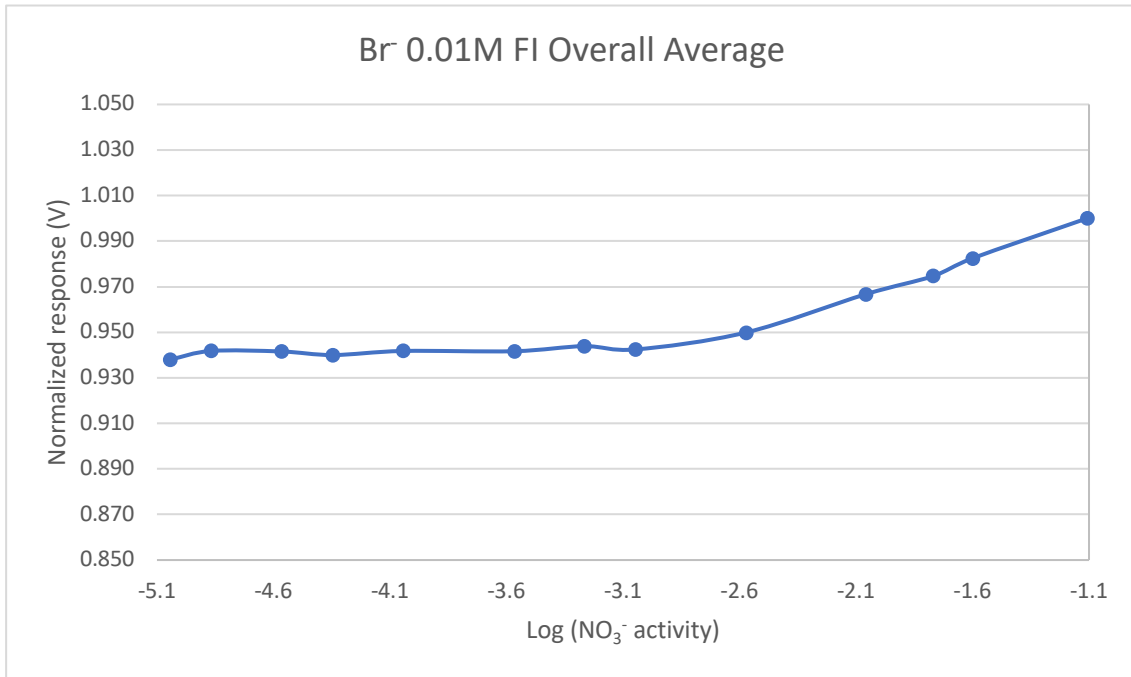


Figure 41. Bromide 0.01M Fixed Interference.

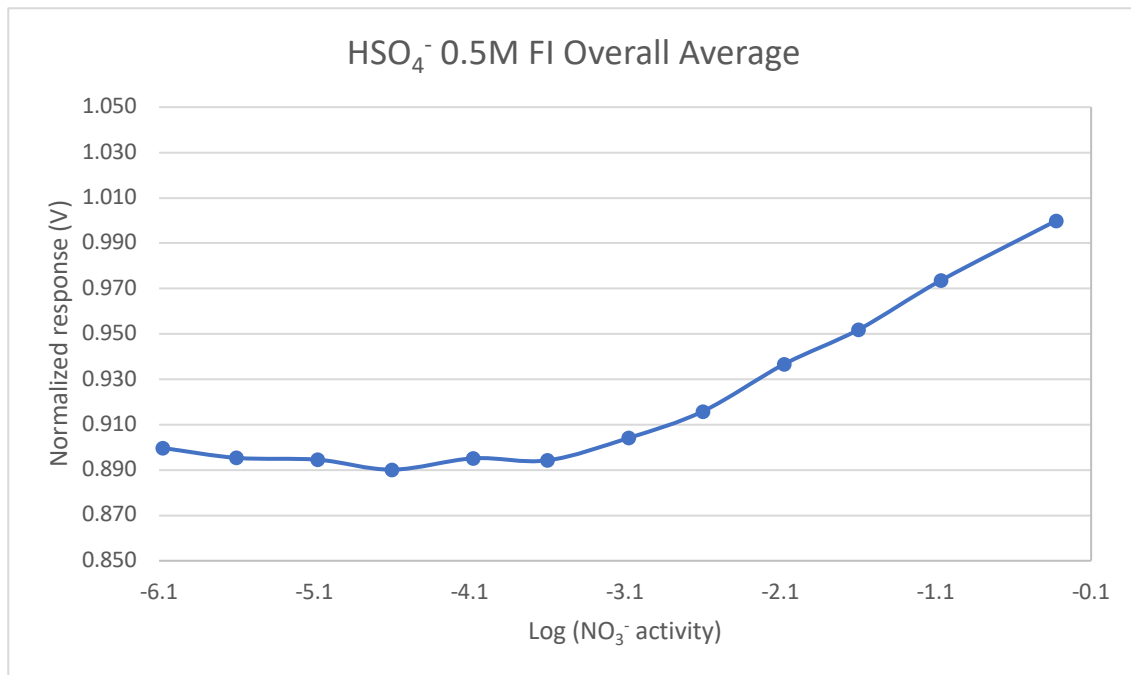


Figure 27. Sulfate 0.5M Fixed Interference.

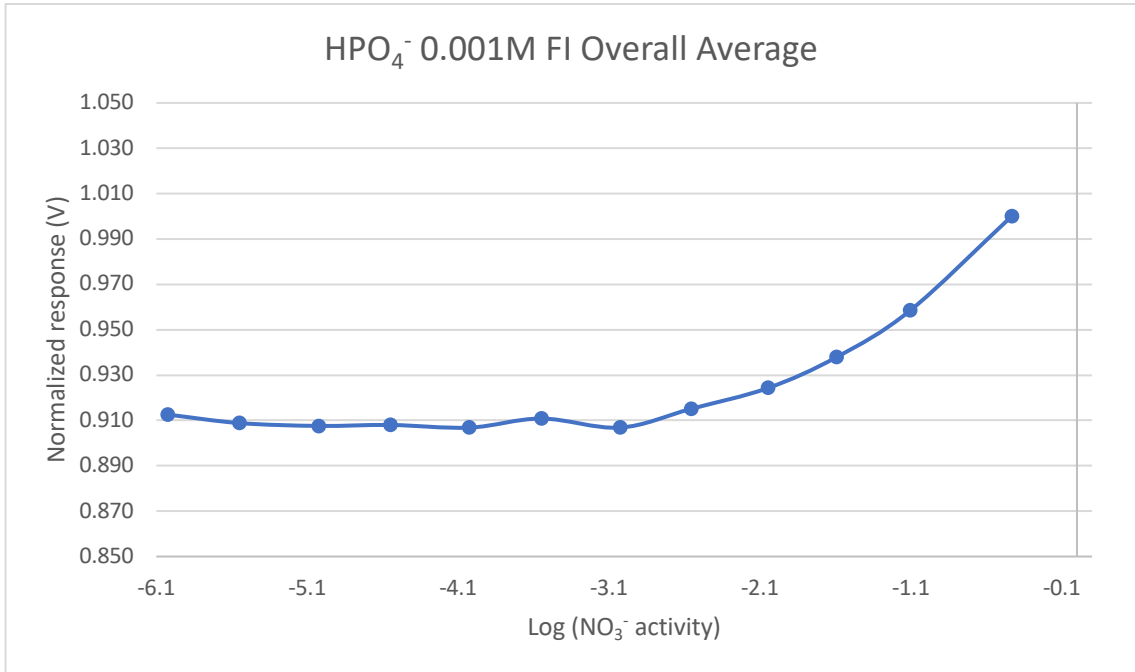


Figure 28. Hydrogen Phosphate 1mM Fixed Interference.

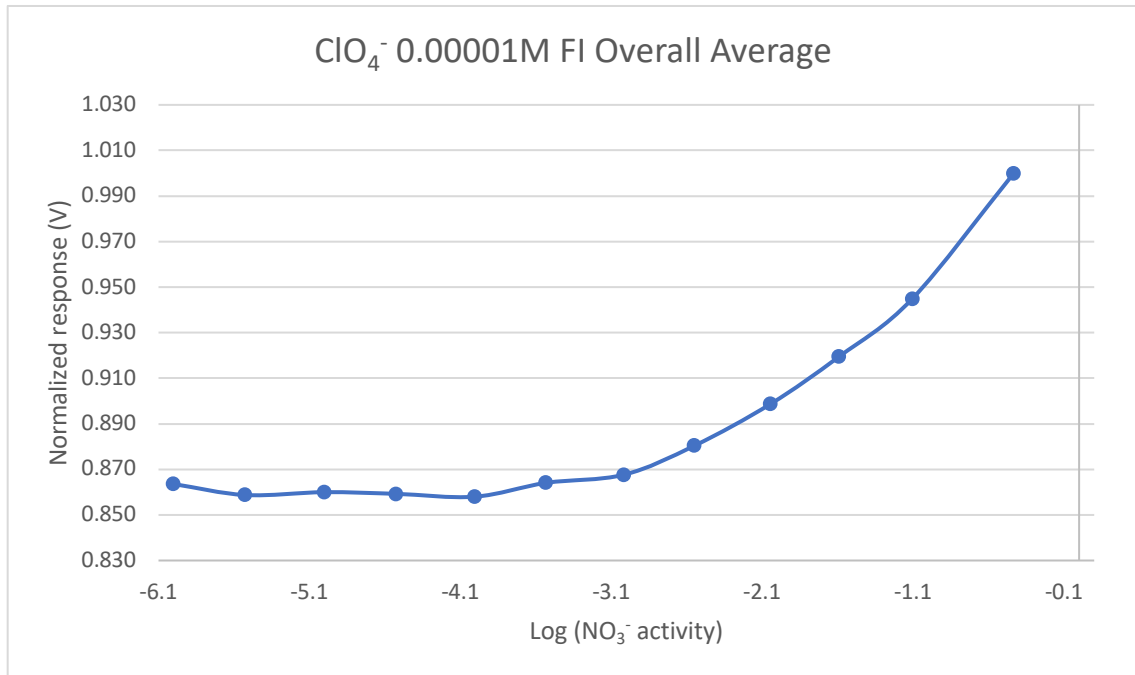


Figure 29. Perchlorate 0.01mM Fixed Interference.

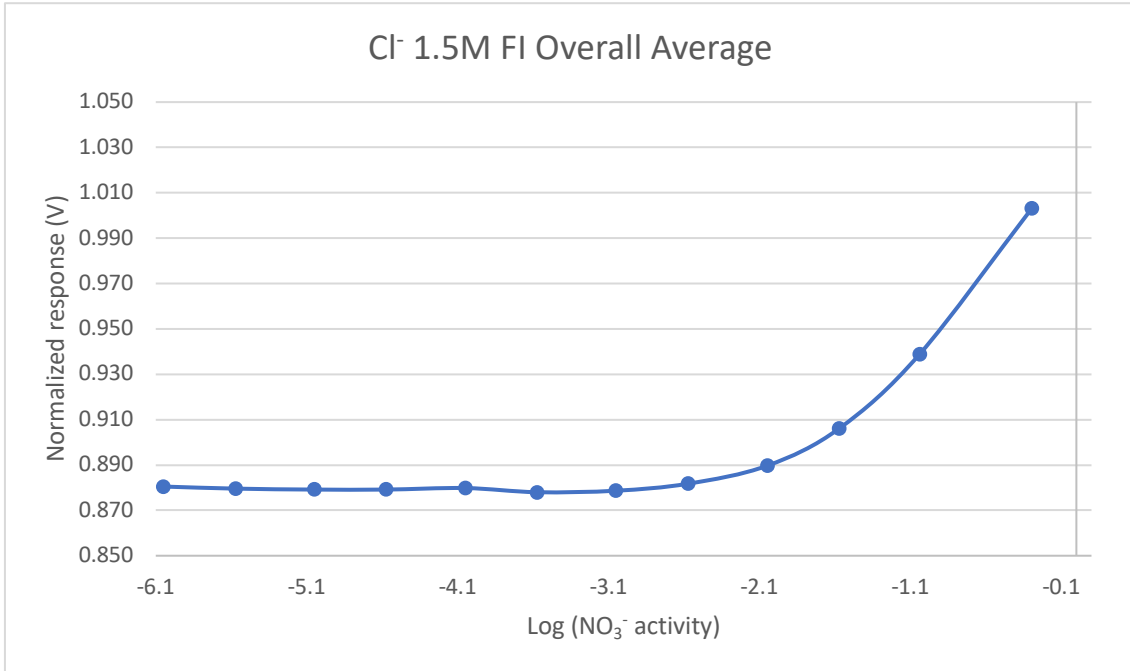


Figure 30. Chloride 1.5M Fixed Interference.

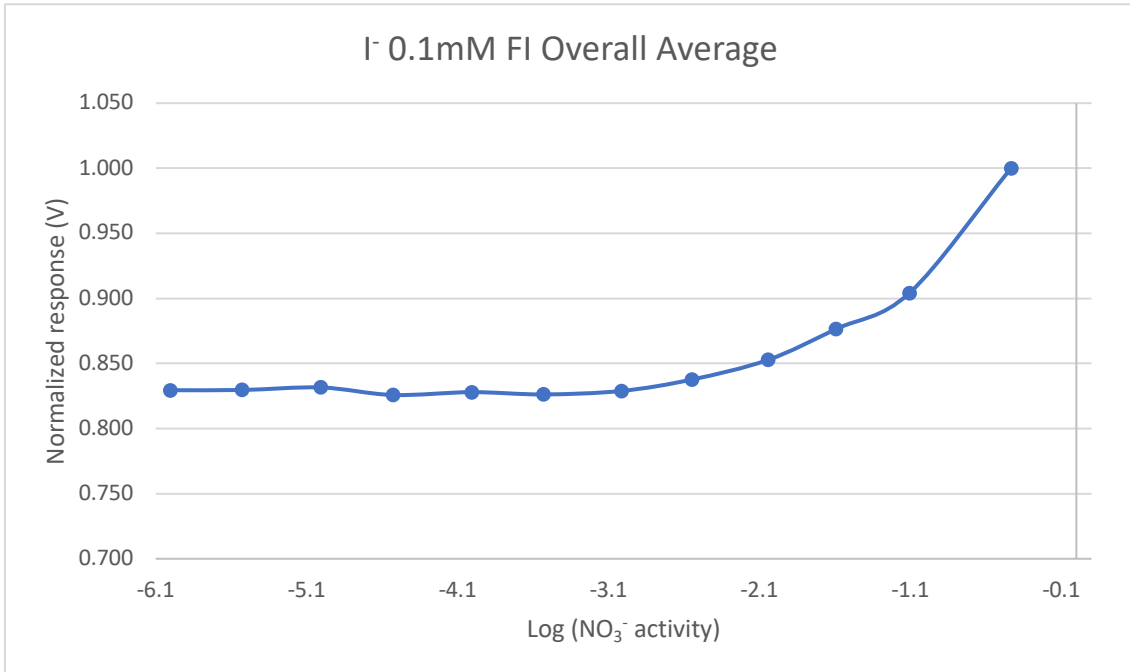


Figure 31. Iodide 0.1mM Fixed Interference.

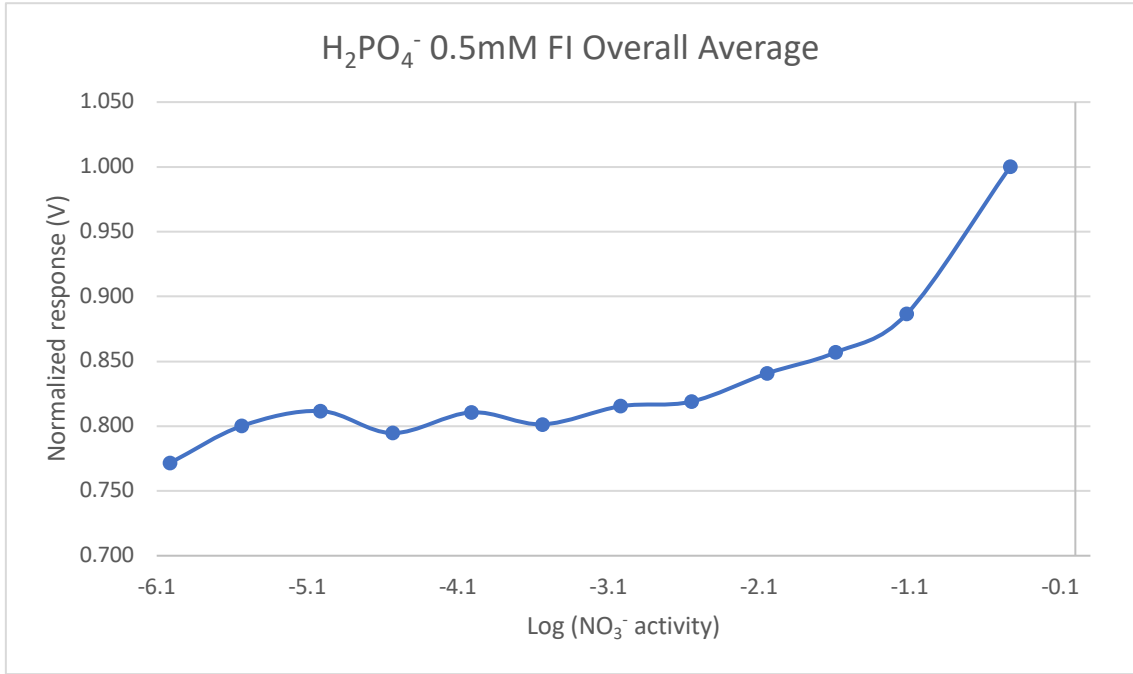


Figure 32. Dihydrogen Phosphate 0.5mM Fixed Interference.

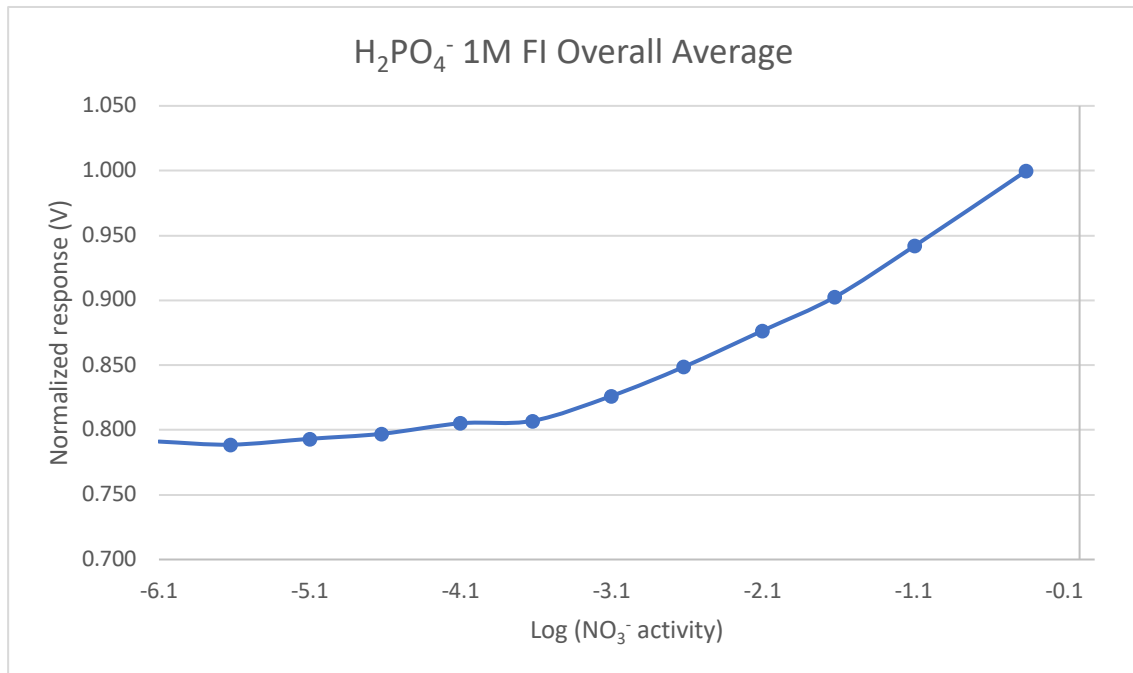


Figure 33. Dihydrogen Phosphate 1M Fixed Interference.

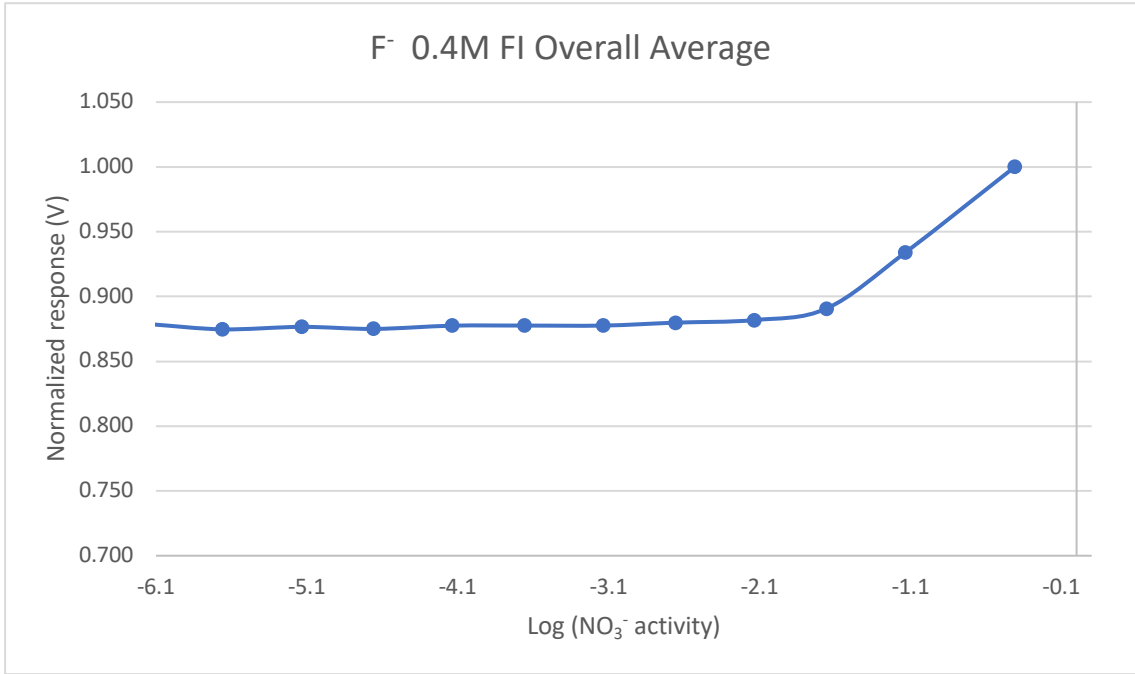


Figure 34. Fluoride 0.4M Fixed Interference.



## REFERENCES CITED

1. Srinivasan, A.; Viraraghavan, T. *International Journal of Environmental Research and Public Health* **2009**, *6* (4), 1418–1442.
2. Eytel, L. M.; Gilbert, A. K.; Görner, P.; Zakharov, L. N.; Johnson, D. W.; Haley, M. M. *Chemistry - A European Journal* **2017**, *23* (17), 4051–4054.
3. Carroll, C. N.; Coombs, B. A.; Mcclintock, S. P.; Johnson, C. A.; Berryman, O. B.; Johnson, D. W.; Haley, M. M. *Chemical Communications* **2011**, *47* (19), 5539.
4. Kaisti, M. *Biosensors and Bioelectronics* **2017**, *98*, 437–448.
5. Hu, J.; Stein, A.; Bühlmann, P. *TrAC Trends in Analytical Chemistry* **2016**, *76*, 102–114.
6. Buck, P. R.; Lindner, E. *Pure & Appl. Chem.* 1994, Vol. 66, No. 12, pp. 2527-2536.
7. Reinhoudt, D. N.; Antonisse, M. M. G. *Electroanalysis* **1999**, *11* (14), 1035–1048.
8. Bergveld, P. *IEEE Sensor Conference Toronto* **2003**.
9. Reinhoudt, D. N. *Sensors and Actuators B: Chemical* **1995**, *24* (1-3), 197–200.
10. Cerreta, M. K.; Berglund, K. A. *Journal of Crystal Growth* **1987**, *84* 577—588
11. Janata, J. *Electroanalysis* **2004**, *16* (22), 1831–1835.
12. Bergveld, P. *Sensors and Actuators B* **2003**, *88* 1–20
13. Harris, S. M.; Nguyen, J. T.; Pailloux, S. L.; Mansergh, J. P.; Dresel, M. J.; Swanholm, T. B.; Gao, T.; Pierre, V. C. *Environmental Science & Technology* **2017**, *51* (8), 4549–4558.

14. Tresca, B. W.; Zakharov, L. N.; Carroll, C. N.; Johnson, D. W.; Haley, M. M. *Chemical Communications* **2013**, 49 (65), 7240.
15. Lehnert, N. "Feeding The World in the 21st Century: Grand Challenges in the Nitrogen Cycle" *NSF Workshop 1550842* **2015**, 1–38.
16. Xie, W. J.; Gao, Y. Q. *The Journal of Physical Chemistry Letters* **2013**, 4 (24), 4247–4252.